
NAPE BULLETIN VOL. 29/2 NOVEMBER, 2020 (ISSN 2734-3235)

NIGERIAN ASSOCIATION OF PETROLEUM EXPLORATIONISTS

SINCE 1975

NIGERIAN ASSOCIATION OF PETROLEUM EXPLORATIONISTS

An International Geoscience Organisation

# NAPE Bulletin

VOL. 29/2 NOVEMBER, 2020 (ISSN 2734-3235)

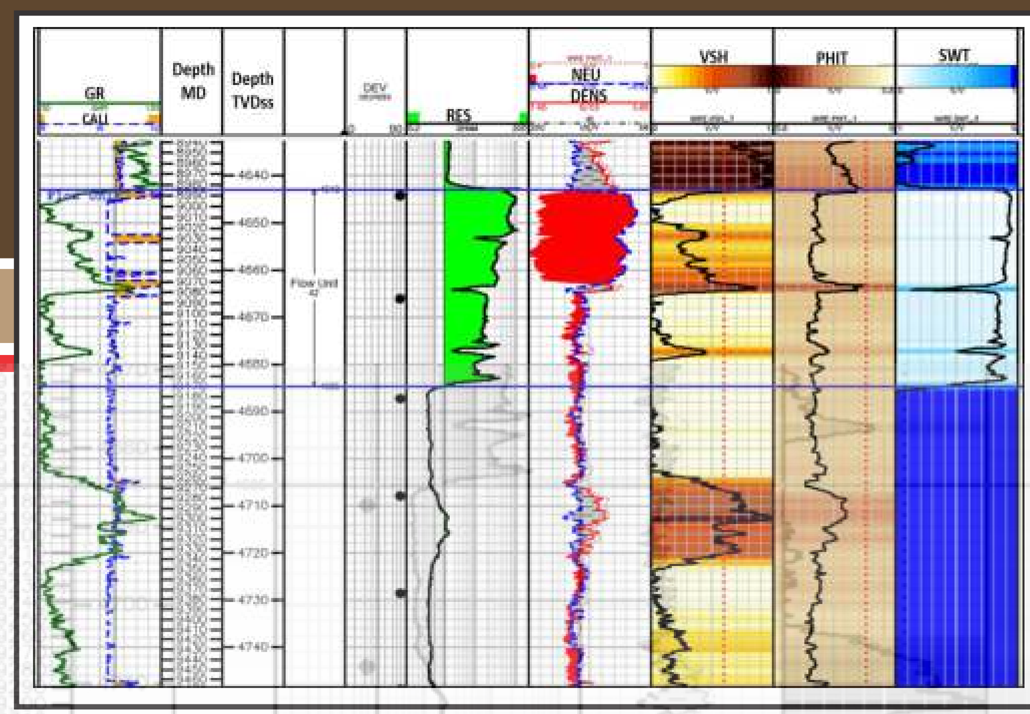


*Our ideas find Oil and Gas*

# C O N T E N T S



**COVER PHOTO EXPLANATION:**
Archie SWT over Study Reservoir Interval
After: Orupabo S.*, Olatunbosun A., Hoda N., Zhou J
Mobil Producing Nigeria Unlimited

# EDITORIAL POLICY AND INSTRUCTION TO NAPE BULLETIN AUTHORS

The NAPE Bulletin is designed for the dissemination of information on the geology and associated technology of petroleum, natural gas, and other energy mineral resources.

**ARTICLES**

Articles are papers of major extent and contain detailed geoscientific data that support original interpretations or methods. Article length is not to exceed 40 double-spaced typewritten pages. Otherwise, Special authorization must be sought through the editor. Published papers include, but are not invariably limited to those presented at any of the Association's technical sessions or the annual conference.

**MEMORIALS**

Memorials are not to exceed 800 words. Longer text is subject to approval by the editor.

**MANUSCRIPT REVIEW**

All Articles are reviewed by two or more referees for technical merit, quality of scientific content, and utility of the results for practicing geoscientist. Discussions and replies are reviewed by the Editor. The Editor makes the final decision concerning the acceptance or rejection of a paper.

**MANUSCRIPT PREPARATION**

Manuscript must be typed double-spaced in Calibri font 11. Please send in a CD or Flash Drive, one original, and 3 photocopies of the manuscript and five photocopies set of the figures to the Editor-in-Chief, NAPE Secretariat, House 47A, Femi Okunnu Rd, Estate Phase 1, Lagos. Send the revised manuscript and any tables and/or computer-generated figures on CD/Flash drive using the following guidelines:

Copy text file in original application

Save graphic file in original application

Indicate disk format and name of application (see below)

Write names used on CD/Flash drive and last name of senior author on label

**MANUSCRIPT PARAMETERS**

Use metric units or measure with English unit equivalent in parentheses if needed.
Laboratory measurement do not require conversions.
Do not use abbreviations except for units of measure.
Cite figures in numerical order.
Cite all references and include complete information for each citation in References Cited section.
Abstract should not be longer than 25 lines.

**REFERENCE FORMAT**

References are ordered alphabetically: In case of multiple listings by the author(s), references are ordered by date (earliest first) and then alphabetically.

Single author journal article: Author's last name, Initials, year title of paper (capitalize only proper nouns): full name of journal, v.x.p. Xx-xx.

Computer programs published in Journals: Author's last name, Initials, year, program title: full of journal, v x p. xx-xx.
Computer programs on disk: organization name, year, program name, version number: city of distributor, name of distributor.

We do not cite work submitted or in preparation: these works are cited as personal communication (e.g. S Jonas, 1990, personal communication within text only).
Units

Measurement should be in metric (S.I) units intext and in Illustrations or metric with Imperial equivalent in parentheses.

**MANUSCRIPT SECTIONS**

Manuscript should be organized as follows:

Title

Author(s) and address(es)

Affiliation(s)

Acknowledgments, if included

Abstract (summarizes paper, approximately 250 words, 25 typed lines)
Text (use headings and no more than two classes of sub headings)

Appendix(es), if included

References Cited

Figure captions (listed on a separate sheet) and NOT **'ENCLOSURE'** or **'PLATES'**

Figures (separate from text)

Tables (separate from text)

**ARTWORK PREPARATION**

Identify by number all figures using pencil, non-reproducing blue Ink, or Indelible Ink.

Do not submit figure larger than 17.8 x 2.9cm (7 x 9 In), expect with permission of the Editor.

Oversize or colour figures are published at expense of author.

Submit colour figure on CD/Flash drive, as print not larger than 20.3 x 25.4cm (8 x 10 in), or as transparencies not larger than 15.2 x 21.6cm (6 x 8.5in) Do not send ink-jet images or colour photocopies.

Indicate orientation and scale on photography or in caption.
Scales/Axes

All figure must include a scale.

Axes must be labelled on graphs.

Scale bar must be included on photo-micrographs. If a slide is submitted, affix scale bar to a photo print of the slide and we will transfer the bar scale to the slide.

Artwork will not be returned.

**PERMISSION/COPYRIGHT**

The author is responsible for obtaining permission to use previously published Illustrations. A letter of permission from the copyright holder must be submitted with the manuscript before editing begins.

**GALLEY PROOF**

No content changes are allowed at galley proof stage.

**COVER PHOTOGRAPHS**

The Bulletin accepts good quality colour slides of geologic interest for the cover. Slides will not be returned.

**REPRINTS**

Senior or corresponding authors should arrange with the editor for reprints. Charges shall be borne entirely by the author(s).

**SUBMISSION TO NAPE OF COMPUTER-GENERATED TEXT AND GRAPHICS**

NAPE uses the printing press for the production of periodicals and thus is limited to the applications and formats locally available. The following are the guidelines for the Computer-Generated Text and Graphics.

**APPLICATION AND FORMATS**

Save text files in their original application as indicated below

**TEXT:**

Microsoft Word

**GRAPHICS:**

Powerpoint (current edition) is recommended

**SPREADSHEET:**

Excel (current version)

**MEDIA REQUIREMENTS**

Please label your CD/Flash drives with your name contents, and the name of the applications(s) used as well as the file format.

If you have any questions about how to submit your computer-generated text and graphics, please contact The Editor-in-Chief, NAPE Secretariat, House 47A, Femi Okunnu Rd, Estate Phase 1, Lagos.

**NAPE POLICY ON ACCEPTANCE OF TECHNICAL PAPER FOR PRESENTATION**

It is the policy of **NAPE** to publish papers present at any of its Technical Meetings or Annual Conference. For this purpose, the Association publishes.

(a) The Bulletin of the Nigerian Association of Petroleum Explorationists (ISSN 2734-3235) which contains ttechnical papers presented to the Association during the preceding Association year, solicited papers, and other papers judged suitable for publication in the Bulletin.
(b) Proceedings of the Annual Conference of the Nigeria Association of Petroleum Explorationists (ISSN 07944-1064) which included papers and discussions at the Annual preconference Workshop and Conference.

In pursuance of this policy, interested contributors to **NAPE** technical program note the following:

1. The presenter would ensure the release of any proprietary data in their texts from the relevant authorities.
2. Although **NAPE** prefers original contributions, part published works may be considered for publications.
3. Where an author represents a paper orally to the Association and does not wish to have the paper published for proprietary reasons or others technical reasons, the author should clearly indicate that on this manuscript
4. All papers are sent to Independent reviewers for technical evaluation before publication

**MANDATORY REQUIREMENTS FOR SUBMISSION OF PAPERS**

It is mandatory for authors submits along their papers, the following via the electronic media:

1. A brief bio-profile
2. A passport size photograph

Reprints of papers in this Bulletin are available for a fee from the

**NAPE Secretariat,**
47A, Femi Okunnu Housing Estate,
Lekki Peninsula, Lagos
P.M.B 12598, Marina, Lagos.
Tel:(234)-1-9092143198.
e-mail: infor@nape.org.ng
website: **www.nape.org.ng**

Dr. Christopher Asuquo Jackson
*Editor-in-Chief*

# Editorial Board Members

## NIGERIAN ASSOCIATION OF PETROLEUM EXPLORATIONISTS

47A, Femi Okunnu Housing Estate, Lekki Peninsula, Lagos.
P.M.B 12598, Marina, Lagos.
Tel: (234)-1-9092143198.
E-mail: info@nape.org.ng Website: **www.nape.org.ng**

## 2019 / 2020 NAPE EXECUTIVE COMMITTEE

| | |
|---|---|
| **Mr. Alex Nachi Tarka,** FNAPE<br>President | Nigerian National Petroleum Corporation-NPDC, Benin City. |
| **Mr. Abiodun Ogunjobi**<br>Vice-President | New Cross Petroleum Limited, Lagos. |
| **Mrs Patricia Ochogbu,** FNAPE<br>President-Elect | ExxonMobil, Lagos. |
| **Mr. Emmanuel Egbele**<br>General Secretary | Total E & P Nigeria Limited, Lagos. |
| **Mr. Charles Otoghile**<br>Assistant Secretary | SCHLUMBERGER, Lagos. |
| **Mr. Ogunjemiyo Esan Mascot**<br>Treasurer | Nigerian National Petroleum Corporation-NAPIMS, Lagos. |
| **Dr. Anthony Ofoma**<br>Financial Secretary | Halliburton Energy Services Nigeria Limited, Lagos. |
| **Dr. Christopher Asuquo Jackson**<br>Editor-in-Chief | PetroVision Energy Nigeria Limited, Lagos. |
| **Mr. Abdullateef Amodu**<br>Publicity Secretary | Chevron Nigeria Limited, Lagos |
| **Dr. Juliet Emudianughe**<br>Assistant Editor-in-Chief | Federal University of Petroleum Resources, Effurun. |
| **Mr. Ehi Bazuaye**<br>Abuja Chapter Coordinator | Nigerian Agip Oil Company Limited, Abuja |
| **Mr. Emo Dayetuawei**<br>Port-Harcourt Chapter Coordinator | Maritime Support Services Ltd, Port Harcourt. |
| **Mr. Wilson Osung**<br>Warri Chapter Coordinator | Petroleum Training Institute, Warri. |
| **Mr. Edward Ozah**<br>Benin Chapter Coordinator | Nigerian National Petroleum Corporation-NPDC, Benin City. |
| **Dr. Ekere Akpan**<br>Uyo / Calabar Chapter Coordinator | Universal Energy Resources Limited, Uyo. |
| **Dr. Abimbola Adewole Durogbitan**<br>UK / Europe Chapter Coordinator | AMNI International Petroleum Development Company, Lagos. |
| **Mr. Oyebamiji Ajibola,** FNAPE<br>Immediate Past President | Nigerian Agip Oil Company Limited, Abuja. |
| **Dr. Emmanuel Maduawia**<br>UAP Chairman | First E & P Development Company Limited, Lagos. |

NIGERIAN ASSOCIATION OF PETROLEUM EXPLORATIONISTS

# ONLINE MEMBERSHIP REGISTRATION PROCEDURES

The Nigerian Association of Petroleum Explorationists (NAPE) is pleased to inform you that all categories of membership registration, upgrade of membership status, checking of payment record, payment of annual due and lots more can now be done online.

**1. ONLINE INDIVIDUAL MEMBERSHIP ADMISSION**
Are you a geoscientist or a professional of related field? You can become a member of NAPE easily by following the procedures below to complete the online individual membership admission form;

**ACTIVE MEMBERSHIP:** Membership in this category is opened to any person engaged in the practice or teaching of the geosciences or petroleum related science; provided he/she holds at least a Bachelors' Degree from an educational institution of acceptable academic standards. This is in addition to at least three years of working experience ( post NYSC) in the practice or teaching of the geosciences or petroleum related science. Credit for experience can be counted as follows: Holder of Master Degree - one (1) year; Doctorate Degree - two (2) years.

***Amount at Registration: N10, 000.00***

**JUNIOR MEMBERSHIP**: In this category of membership, the applicant must be a graduate with a major in any of the geosciences or petroleum related science, who has completed his/her NYSC and with less than 3 years working experience (post NYSC) in oil and gas industry or in related field.

***Amount at Registration : N7, 000.00***

**ASSOCIATE MEMBERSHIP:** Kindly note that an applicant in this category of member ship could be any person not qualified for any other class of membership but is a graduate of an educational institution of acceptable academic standards with major studies related to, or generally associated with geosciences or petroleum related science. The Executive committee may decide waive degree requirements for this class of applicant if the need arises.

***Amount at Registration: N10, 000.00***

**STUDENT MEMBERSHIP:** An applicant of this category must be an undergraduate pursuing a major in any of the geosciences or petroleum related science.

***Amount at Registration : N2, 000.00***

**Method of Application and Requirements:** For all in the individual membership category, kindly click on the link **http://members.nape.org.ng/application/new/** to log on to the new NAPE Membership Application page. under "apply now" click on "individual membership" to complete the online Individual membership Admission form.

Be informed that all applicants for ACTIVE, JUNIOR or ASSOCIATE membership would be requested to upload the following for the completion of membership admission form;

1. Comprehensive Curriculum Vitae (CV)
2. Degree Certificate(s)
3. NYSC discharge certificate
4. Passport sized photograph
5. Evidence of bank payment slip.

Please note that the size of each upload document must not exceed 1MB.

Applicant will also be required to submit the particulars of two referees, who will endorse his/her application.
The required particulars are: Referees Name, Membership ID (i.e NAPE Registration Number). Note that the referees MUST be registered Active members of NAPE with their functional e-mails registered on the NAPE members' portal

All applicants for STUDENT membership category would be requested to upload the following for the completion of the membership form;

1. School identity card or School admission letter (if school ID is not available)
2. Passport size photograp
3. Evidence of bank payment slip

Note that size of each upload document must not exceed 1MB

A student membership applicant will be required to submit the particulars of TWO referees who will endorse his/her application. The particulars of the referees should entail; name, membership ID (NAPE Registration number).The referees MUST be registered ACTIVE members of NAPE and at least one of them MUST be the applicant's Department Lecturer or NAPE-UAP Faculty adviser with a functional email registered on the NAPE members' portal.

**2. CORPORATE MEMBERSHIP ADMISSION**

Any company or institution registered in Nigeria and engaged in the practice or teaching in the areas of Oil and Gas, Energy, Mineral exploration and petroleum activities; either as an operator, shareholder or service company, training or financial institution may apply for corporate membership.

**Method of Application and Requirements:**
kindly click on the link
**htt://members.nape.org.ng/application/new/** to log on to the new NAPE membership Application page.
Under "apply now" click on corporate membership admission form.

Be informed that applicants would be requested to upload the following for the completion of the membership admission form.

1. DPR permit or corporate Affairs Commission Certificate (in the absence of DPR permit)

2. Company profile detailing list of key executive, business endeavor, specialization area, past and current jobs (in case of service companies)

**Amount at Registration:** Ninety thousand Naira (N90, 000.00) which covers the following;

| | |
|---|---|
| 1. Application fee | - N10,000.00 |
| 2. Registration fee | - N30,000.00 |
| 3. Corporate Annual Dues | - N50,000.00 |

**Mode of Payment:**
for all categories of membership, all payment should be made to NAPE membership Account with details below;

**Bank Name:** United Bank of Africa (UBA) Plc
**Account N0:** 1005158666
**Account name:** Nigerian Association of Petroleum Explorationists (NAPE)

The name of the depositor written on the bank deposit slip must be the same as the name of the registered member or corporation. For individual, it should be surname first. Deposit slip or bank draft should be scanned and emailed to NAPE secretariat for confirmation and a NAPE receipt will be issued subsequently. Thereafter, a membership certificate will be issued and this authenticates applicants' membership.

**3. ANNUAL DUES AND CONFERENCE REGISTRATION**

For online payments for association membership annual dues and conferences using InterSwitch Debit Cards ( Verve and Naira MasterCard), go to the NAPE onlinePAY portal: (http://payments.nape.org.ng/)
make use of links below for more information:
1. How It works / Getting Started
(http://payments.nape.org.ng/howitworks.php)
2. Frequently Asked Questions
(http://payments.nape.org.ng/faqs.php)
3. Previous and current Fee Schedule
(http://payments.nape.org.ng/fees.php)

**4. ONLINE INDIVIDUAL UPGRADE OF MEMBERSHIP**

For registered members in the student or Junior category, seeking to upgrade membership, visit the members ONLY portal link http://members.nape.org.ng log on to your membership accounts with your ID and password to complete application form and online payment. For details on this, contact Head of Membership Services, Mr. Tunde Adedeji, tunde.a@nape.org.ng or call + 2349092143198.

Please visit our website **"www.nape.org.ng"** for more information on NAPE.

*For further enquiries, kindly contact*
Nigerian Association of Petroleum Explorationists
47A, Femi Okunnu Housing Estate
Lekki Peninsula.
Tel: (234)-1-7731539; +2349092143198
E-mail: osuagwu.l@nape.org.ng

NIGERIAN ASSOCIATION OF PETROLEUM EXPLORATIONISTS

SINCE 1975

# The SHELFAL Collapse Play – A Case Study from a Producing Field in the Niger Delta, Offshore Nigeria

**Ndianefo U. K.*, Bassey N. E. and Onyido I. M.**
*Mobil Producing Nigeria Unlimited

## ABSTRACT

The Shelfal Collapse Play ranks as one of the least understood and understudied plays in the petroleum industry. Interestingly, this play has one of the most unique, distinguishable and predictable genetic process associations that translates to a potential set of very distinctive prospects comprising good quality reservoirs and traps, as clearly observed and described in the Abang and Oso fields, offshore Niger Delta. The collapse of a shallow marine prograding wedge rich with sandy deposits at the Oso Field, led to the emplacement of sand-rich gravity deposits in favorable trapping configurations at the Abang Field. Instability caused by high rates of sediment supply without commensurate accommodation downdip and consequent loading of shelf-edge deltaic sediments on a decollement surface or zone is one of the leading mechanisms of this type of shelfal collapse. Multiple depositional styles have been observed on seismic within the accommodation created by the collapse. They typically involve the deposition of slumps and slides recognized as concave upwards rafted geometries in cross-section, passing downdip into debris flow identified as mostly chaotic and transparent seismic facies, followed by a capping succession of turbiditic deposits recognized by channel map patterns on amplitude extractions. A case study from the Abang Field using seismic and well logs will throw more light on these clear identification criteria, which can be used in finding similar prospects within the geologic record. The resourceful nature of this play will be highlighted by the Abang wells which produce oil from both the turbiditic and debrite facies with end of field life recovery factor estimated to be between 0.35 and 0.60.

**Keywords:** Shelf collapse, offshore, fairways, reservoirs, amplitude Extraction, debris flow, turbidites.

## INTRODUCTION

Shelfal collapse plays have been rarely identified or described in the Niger Delta Basin. Where they have been identified, explored and exploited, they play host to significant amount of hydrocarbon reserves due to a favorable conflagration of play elements especially relating to charge, traps and reservoir presence.

Unlike the Niger Delta Basin, detailed published descriptions exist of shelf margin collapse events from other basins around the world (Almagor, 1980; Lee *et al.,* 1991; Field *et al.,* 1982; Edwards, 1990; Edwards, 1991; Normark and Gutmacher, 1988; Edwards, 2000). Of particular interest is the description of retrograde failed shelf margins by Edwards (2000). What is unique about his work is the detailed description of key features and genetic models of retrograde shelf margins (caused by collapse) using examples from the Northern Gulf Coast Basin (USA), thus providing an understanding of the genetic relationships and recognition criteria that makes the shelfal collapse play a prolific one. He summarized the paucity of data conundrum when he said – "relatively few publications have described features that are unmistakably of the type covered in this paper. This is partly because most recent published studies are regional in scope and posited that older publications did not recognize them as distinct feature." This regrettably remains the case today, especially in the Niger Delta Basin. For example, the Qua Iboe Shelf Collapse – a large regional scale shelfal collapse within the Niger Delta Basin covering about 6000 sq.km with more than six (6) billion barrels of Oil Originally in Place – has very little detailed description and recognition criteria (Krukrubo et al., 2013; Onwude et al., 2013) in the public domain. The paucity of published detailed descriptions of this collapse could be related to its very large-scale nature (spanning multiple fields), making it difficult to have a synthesized description of all the architectural elements within the collapse.

Our study will describe a much smaller Tortonian Shelfal Collapse Play (The Abang Shelfal Collapse) comprising the Abang Field Discovery in the Niger Delta Basin, offshore Nigeria (Figure1). We intend to use this study to highlight the genetic features within the Abang Collapse



The authors wish to appreciate the Nigerian National Petroleum Corporation for approving the release of the material presented in this work as well as Mobil Producing Nigeria Unlimited for permission to present this work

and to describe the unique trapping configurations possible with similar plays. Wells and production data will also be used to highlight how prolific the deposits that constitute the reservoirs are. Ultimately, these observations can be scaled and used as analogues in similar or larger regional studies.

Rapid sedimentation (sediment supply >> accommodation) of the Benin and Agbada formations over the under-compacted and mobile shales facies of the Akata Formation is the leading cause of deformation within the delta (Adegoke *et al.,* 2017). This is evident in the abundance of structure building growth faults and shale diapers characteristic of syn-sedimentary deformation.

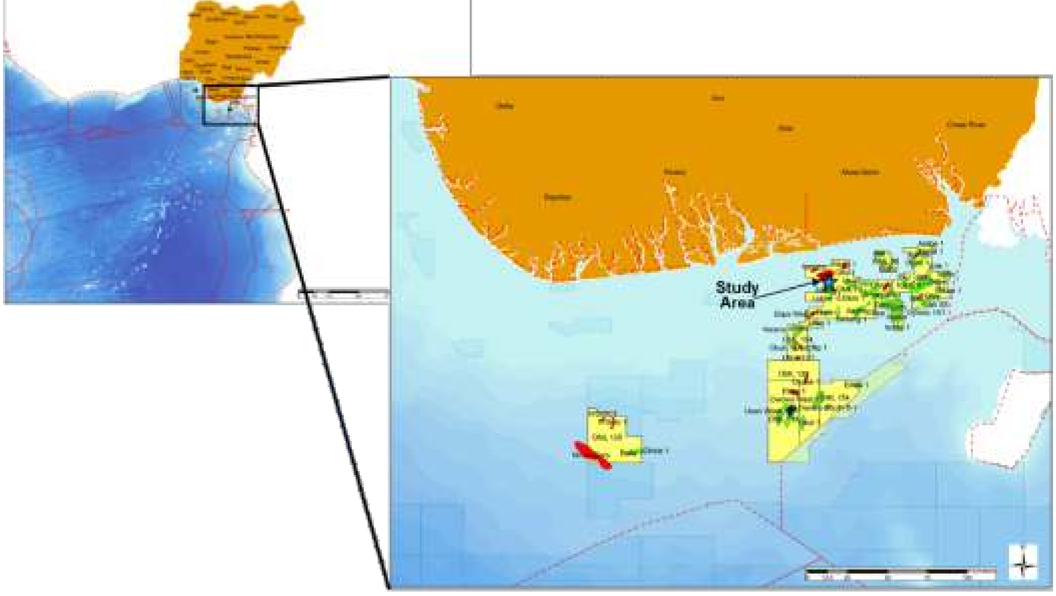


**Figure 1:** Location Map showing the Study Area within the MPN-JV Acreage, off the Coast of Nigeria.

## Geology Background

The Tertiary Niger Delta is one of the world's largest and extremely prolific hydrocarbon province (Doust and Omatsola, 1990; Haack et al., 2000). It is listed in the "Top 25 Global Super Basins" with cumulative production and remaining oil and gas reserves exceeding five (5) billion barrels of oil equivalent (Sternbach, 2018) and overlies an area that covers over 256,000 sq.km (Adegoke et al., 2017).

The origin of the Niger Delta Basin is tied to the South Atlantic Rifting that led to the separation of the South American and African Plates (Short and Stauble, 1967; Whiteman, 1982; Doust and Omatsola, 1990). This led to the deposition of over 12 kilometers of thick Tertiary deltaic sediments characterized by prograding diachronous facies of continental to deep marine facies. These sediments are popularly grouped into 3 lithostratigraphic units (Dessauvagie, 1972; Reijers *et al.,* 1997; Whiteman, 1982) – the Akata Formation (marine mud, slope and basin floor turbidites), the Agbada Formation (Paralic - Shoreface, Lagoon, Distributary Channel, and Transgressive sands) and the Benin Formation (Continental Fluvial sands).

The rapid sedimentation rates, coupled with the dominance of fine-grained sediments towards the medial to distal portions of the delta has contributed to the formation of 3 main structural domains – the extensional, the translational and the contractional domains. In special cases, the instability associated with rapid sedimentation rates over the shelf-slope break can be the trigger for shelfal collapses which are sometimes aided by existing zones of weakness.

This study will focus on the Abang Shelfal Collapse (Figure 2) located within the extensional domain and of Tortonian age in the Abang-Oso Field area (Figure 3).

## METHODOLOGY AND RECOGNITION CRITERIA

Several architectural elements have been identified within the Abang Collapse (Figure4), consistent with descriptions and observations made by Edwards (2000) from the Northern Gulf Coast Basins (the Hackberry Collapse in particular). Identification of these elements were aided by 3D seismic data, well and production data within the Abang-Oso area Collapse

The Abang Collapse is a relatively small scale collapse that covers an approximate area of 85 sq.km. It occurred in the Tortonian and its base (a discontinuity surface) can be observed on 3D seismic data as mappable arcuate-shaped decollement or truncation surface (Figures 4 & 5). The decollement surface is generally coincident with the Tortonian 3 defined Sequence Boundary (Unconformity) in the downdip areas while its headscarp (Mosher et al., 2010) is easily recognizable as the boundary between semi-continuous/continuous reflectors (outside the Collapse) and chaotic/discontinuous reflectors (within the Collapse) (Figure 5). According to Edwards (2000), this is a key geometrical feature of a retrograde failed shelf margin and can sometimes be misinterpreted as a fault. The collapse is believed to have been initiated during the Tortonian Lowstand due to sediment loading within the Oso shelf edge delta, north of Abang. The high sedimentation (sand-rich) rate at Oso coupled with the presence of a possible plane of weakness, created conditions that allowed for the collapse of the Tortonian 3 (and possibly the Upper Tortonian 2) deposits. An approximate volume of thirty-nine cubic kilometers (39cu.km) of sand rich sediments is believed to have collapsed into the bathymetric low, and transported downdip via gravity flow processes.

**Rotational Slump Blocks**

Rotational Slump blocks as defined by Easterbrook (1999) have been observed within the Abang Collapse manifesting as detached blocks of rock which slid along a concave upward slip surface with rotation about an axis parallel to the slope. These blocks are more prevalent closest to the headscarp (Mosher et al. 2010; Figure 4) and rest on the unconformity surface, and in some cases, on other slump blocks within the collapse. In general, the identified scarps indicate a stairstep pattern of displaced blocks. Though unpenetrated in Abang, it is believed that these slump blocks are sand-rich due to the close proximity to the paleo sand-rich shelf-edge delta that initiated the collapse at Oso, as well as the presence of sand prone facies in the downdip debris flow (Figure 4). Edwards (2000) described similar slump blocks in the Gulf Coast Basin as comprising shallow water deposits of interbedded sands and silty shales, supporting the plausible interpretation of a collapsed shelf edge delta.

**Debris Flows**

Downdip of the slumps, debris flows (Lowe, 1979) or

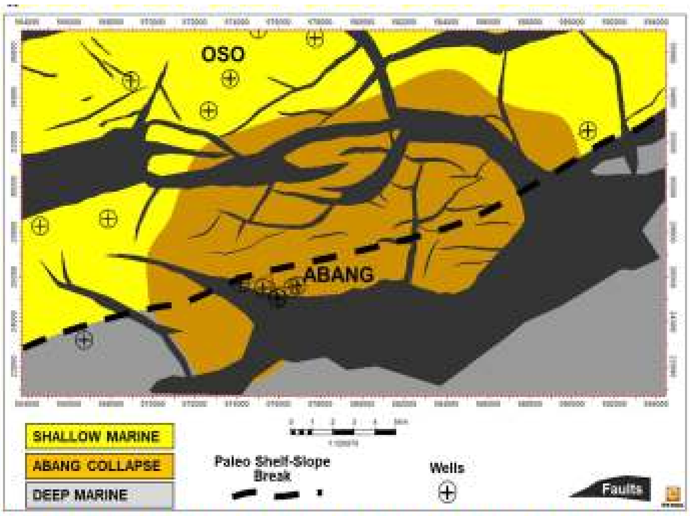


**Figure 2:** Outline of the Abang Shelfal Collapse.

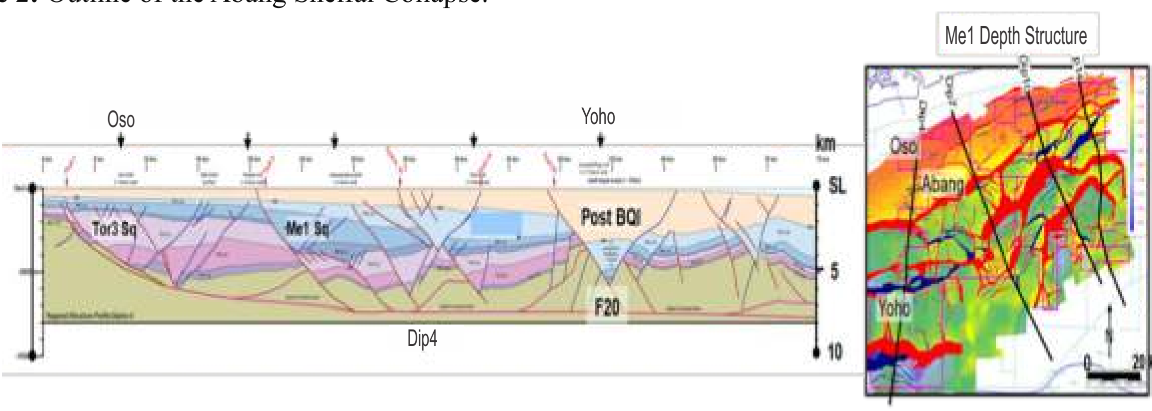


**Figure 3:** Dip-section highlighting the Location of the Oso-Abang Area within the Extensional Domain.

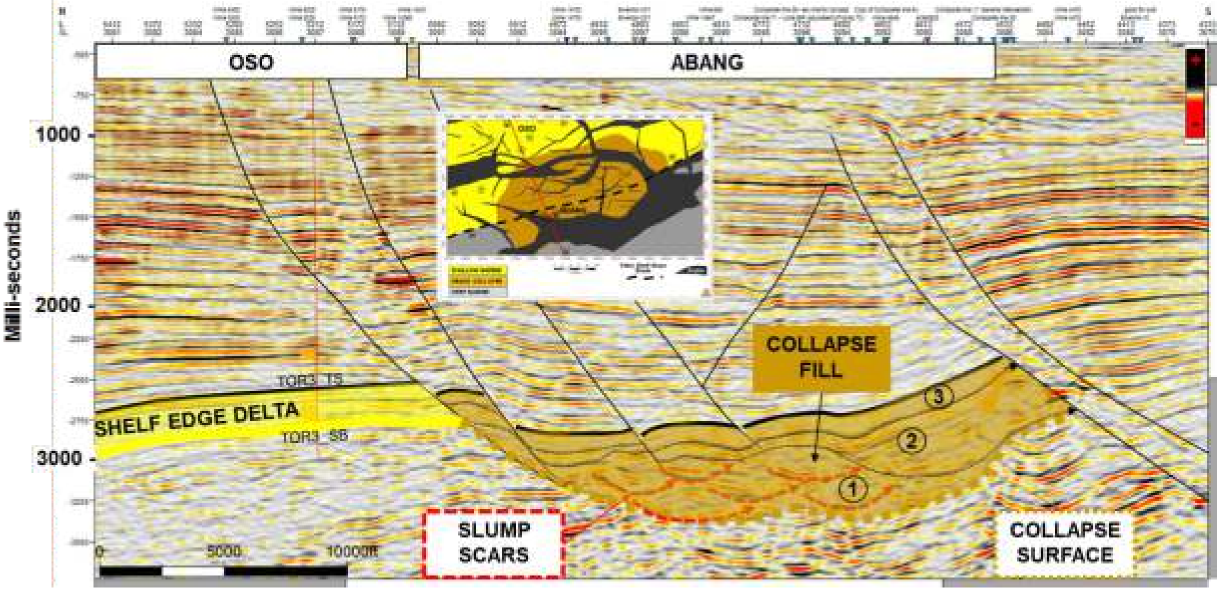


**Figure 4:** Seismic section highlighting the main architectural elements that make up the Abang Collapse (1. Slump Blocks; 2. Sandy Debrites; 3. Turbidites).

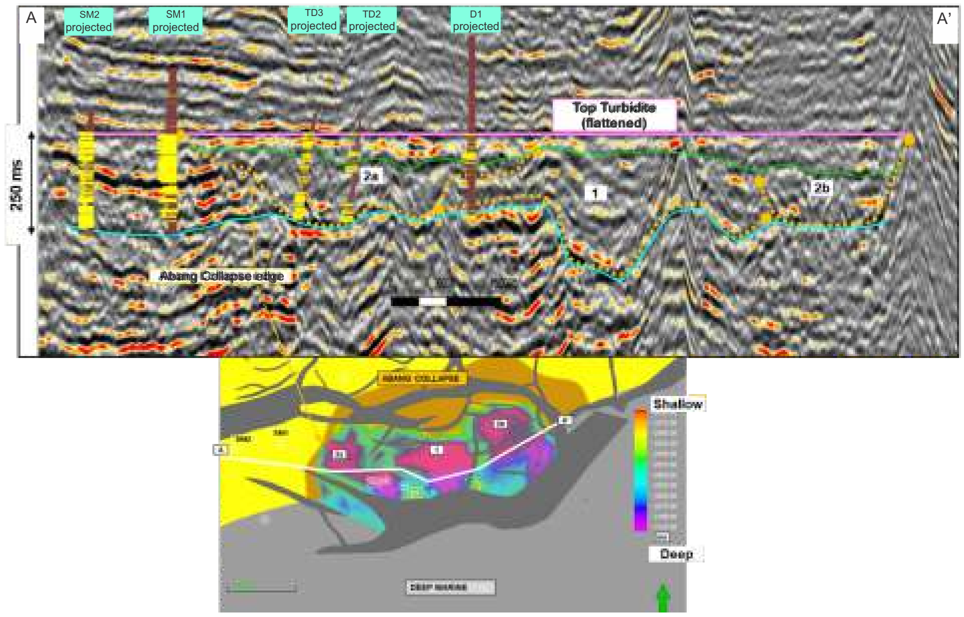


**Figure 5:** Seismic section showing boundary between semi-continuous/continuous reflectors (outside the Collapse) and chaotic/discontinuous reflectors (within the Collapse).

slope aprons (Edwards, 2000) were deposited. These partially fluidized flows are a manifestation of the bathymetric low (deepwater) created by the evacuation of strata during the collapse. They can be erosive due to the high shear stress associated with their transportation and are observed to lie side by side with deepwater hemipelagic/pelagic deposits (Haughton et al., 2003; Amy and Talling, 2006; Sumner et al., 2009). In Abang, three major debris flow fairways have been observed (Fig. 6). These fairways were recognized via a combination of depositional profiles, seismic facies character and well data. Subtle thickness variations highlights fairways characterized by longitudinal thicks. On seismic they are characterized internally as transparent to chaotic seismic facies (Figure 5). Well data from one of the fairways confirm significant high quality sand deposition (Fig. 7). The considerable net sand deposition within the debris flow deposit in Abang is likely tied to the up-slope presence of a shallow marine sand-rich shelf edge delta at Oso (Fig. 4). This, in combination with the Lowstand setting at this time contributed to creating sediments fairways favorable to sand-rich deposits by gravity processes.

continuous to continuous reflections with clear linear amplitude trends originating from the headward portions of the collapse (Figure 7). It is also possible that, further down the depositional profile (outside the study area), the debris flow deposits transitions to turbidity flow deposits (Haughton et al., 2003; Amy and Talling, 2006; Sumner et al., 2009).

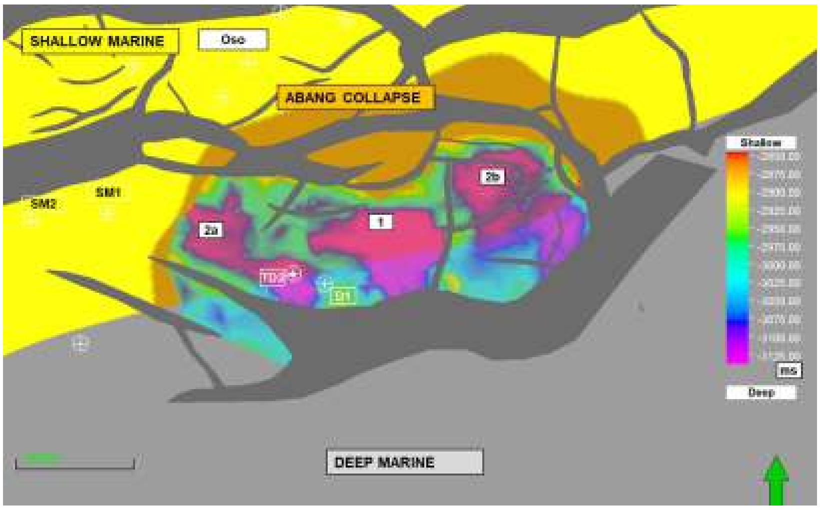


**Figure 6:** Depositional profile of the base of the debritic section interpreted on a flattened seismic volume shows 3 major fairways (1, 2a and 2b) within the Abang Collapse. Fairways 1 and 2b are unpenetrated and are the targets of near term delineation/exploration.

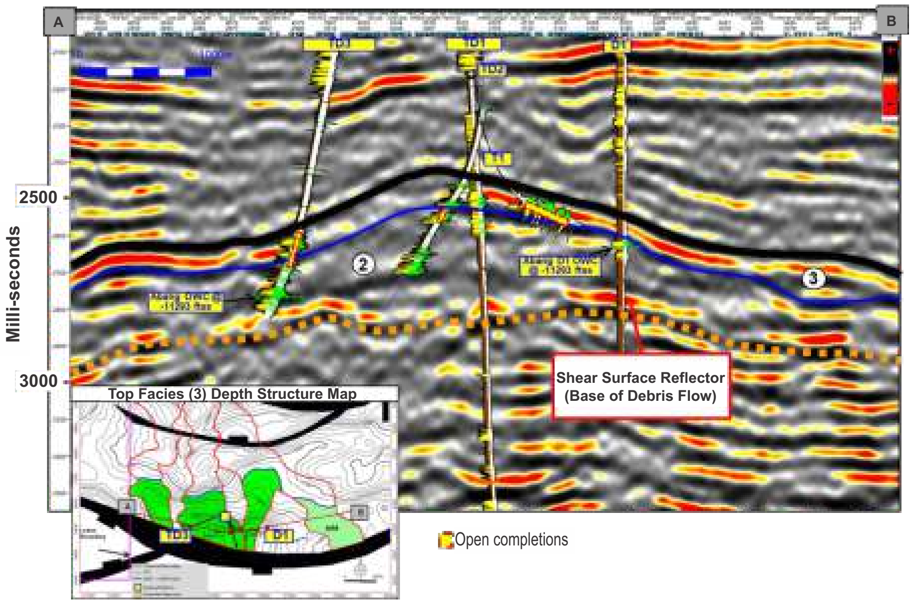


**Figure 7:** Seismic Section showing the Transparent Seismic Facies nature of the sandy debris facies. Well data confirm presence of good quality sand in these transparent debritic facies (2. Sandy Debrite; 3. Turbidites). The Top Facies-3 depth map also shows the outlines of the turbidite facies fairways.

## Turbidites

Increasing levels of fluidization led to the deposition of turbidites. On seismic, these deposits are generally layered above the slump and debris flow deposits and are characterized by relative bright amplitude semi-

## Shelf Deposits

Shelf edge delta progradation past the collapse region led to the deposition of shelfal/deltaic sediments above the Collapse fill. In Abang, this deposition coincides with the late stages of the Tortonian-3 Lowstand when relative sea-

**Table 1:** Reservoir properties of the producing facies in Abang.

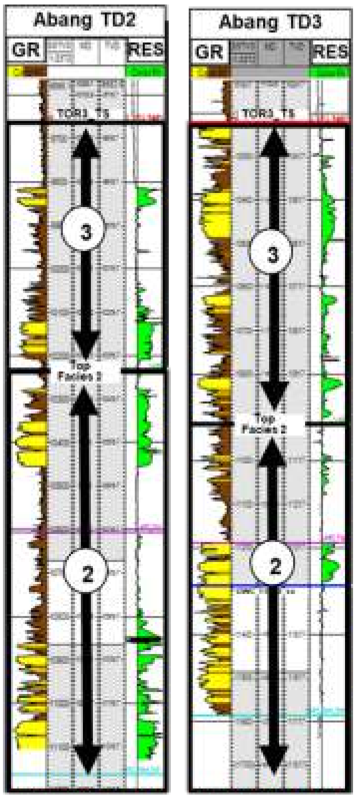


**Reservoir Characteristics**

| | Facies 3 (Turbidites) | Facies 2 (Sandy Debrites) |
|---|---|---|
| Drive Mechanism | • Solution Gas<br>• Weak aquifer support | • Solution Gas<br>• Weak aquifer support |
| Avg NTG | 0.60 | 0.62 |
| Porosity (%) | 27 | 25 |
| Permeability (mD) | 100-500 | 100-500 |
| HC Saturation (%) | 82 | 80 |

level was just beginning to rise. Eventually, the collapse deposits became capped by distal shelf shales on the Transgressive Systems Tract (TST). In Figure 4, the TOR3_TS marks the onset of shelfal deposition.

## RESULTS

The Abang Field (STOOIP in excess of 120 Million Barrels of Oil) was discovered in 1992 and streamed in 2012.

### Reservoir Characterization

As previously described, the Abang Collapse fill comprises slumps, overlain by sandy debrites and turbidites, eventually capped by dominantly muddy shelf deposits. The Abang reservoir comprises 2 main facies – the turbidite facies and the sandy debrite facies. These have reasonably good reservoir properties (Table 1). No penetration of the slump facies has been made yet, while the shelfal deposits are mostly shales.

### Trapping Configuration

The Abang Field is an updip, fault dependent 3 way closure with some lateral stratigraphic trapping observed locally (Figure 7). Pressure data suggest communication across the reservoir bearing sub-units. Contact information from the wells indicate that the hydrocarbon accumulation is constrained by the spill point of the shallowest reservoir sub-unit (Unit 3), though trapped (perched) water as witnessed in Well D1 can occur locally due to local topographic variations (Figure 7).

### Field Production

3 production wells have been drilled till date (Fig. 7). The Abang T1 and TD2 wells are producing from turbidite facies (facies 3); while the Abang TD3 well is producing from the sandy debrite facies (facies 2). The Abang producers have good reservoir properties (Table 1), each producing an average of 7 thousand barrels of oil per day, with more producer wells planned in the near term.

## CONCLUSION

The Abang Collapse presents a rare opportunity to study the geometry and characteristics of the architectural elements that constitute the fill of a relatively small-scale shelfal collapse. Shelfal collapse regions are filled with sediments that have very complex and variable facies distributions. The reason for shelfal collapses have been debated, but a plausible cause associated with this study is one due to shelfal instability from sediment loading and sudden failure by shelf edge deltas. In Abang, the collapse is an arcuate shaped depression that created a bathymetric low for sediments to be funneled via gravity processes (Figure 4).

The initial space is filled by arcuate shaped slump blocks, which transition to debris flow deposits, turbidites and then capped by shelfal sediments as the collapse is eventually filled up. The updip-depositional presence of correlate-able sandy shelf edge deltas (Oso) increases the likelihood of having significant sandy facies with good reservoir properties within the collapse. The Abang debris flow and turbidite facies have good reservoir properties. This is especially note-worthy for the debris flow deposits, whose transparent character on seismic might lead to a shaly facies mischaracterization. Under favorable trapping conditions, these sandy debrites and turbidite facies can hold significant hydrocarbon volumes as evidenced in Abang.

## REFERENCES CITED

Adegoke, O. S., Oyebamiji, A. S., Edet, J. J., Osterloff, P. L., Ulu, O. K., (eds.) (2017). Cenozoic foraminifera and calcareous nannofossil biostratigraphy of the Niger Delta. Elsevier, Netherlands.

Almagor, G., (1980). Halokinetic deep-seated slumping on the Mediterranean Slope of Northern Sinai and Southern Israel. Mar. Geotech.; v. 4; p. 83-105.

Amy, L. A., and Talling, P. J., (2006). Anatomy of turbidites and linked debrites based on long distance (120 by 30 km) bed correlation, Marnoso Arenacea Formation, Northern Apennines, Italy. Sedimentology; v. 53; p. 161–212.

Dessauvagie, T. F. J., (1972). Biostratigraphy of the Odukpani (Cretaceous) Type Section, Nigeria. In: Dessauvagie, T. F. J., and Whiteman, A. J., (eds.); African Geology, Univ. Ibadan, Nigeria; p. 207-218.

Doust, H., and Omatsola, E., (1990), in, Edwards, J. D., and Santogrossi, P.A., eds. Divergent/passive margin basins, AAPG memoir 48: Tulsa, American Association of Petroleum Geologists; p. 239-248.

Easterbrook, D. J., (1999). Surfaces, processes and landforms (2nd ed.). Prentice hall, ISBN 978-0138609580.

Edwards, M. B., (1990). Stratigraphic analysis and reservoir prediction in the Eocence Yegua and Cook Mountain Formations of Texas and Louisiana. In: Sequence stratigraphy as an exploration tool: GCSSEPM Foundation, 11th Annual Res. Conf.; p. 151-164.

Edwards, M. B., (1991). Control of depositional environments, eustacy, and gravity and salt tectonics on sandstone distribution in an unstable shelf edge delta, Eocene Yegua Formation, Texas and Louisiana. Gulf Coast Association of Geological Societies Transactions; v. 41; p. 237-252.

Edwards, M. B., (2000). Origin and significance of retrograde failed shelf margins; Tertiary Northern Gulf Coast Basin. Gulf Coast Association of Geological Societies Transactions; v. L; p. 81-94.

Field, M. E., Gardner, J. V., Jennings, A. E., Edwards, B. D., (1982). Earthquake-induced sediment failures on a 0.25-degree slope, Klamath River Delta, California. Geology; v. 10; p. 542-546.

Haack, R. C., Sundararaman, P., Diedjomahor, J. O., Xiao, H., Gant, N. J., May, E. D., Kelsch, K., (2000). Niger Delta Petroleum Systems, Nigeria. In: Mello, M. R., Katz, B. J. (eds.), Petroleum Systems of South Atlantic Margins. AAPG Memoir; v. 73; p. 213-231.

Haughton, P. D. W., Barker, S. P., McCaffrey, W. D., (2003). 'Linked' debrites in sand-rich turbidite systems – origin and significance. Sedimentology; v. 50; p. 459-482.

Krukrubo, G. J., Nwakwue, J. E., Babafemi, O. A., Young, R. H., Ogunnusi, H. O., (2013). Optimal infill drilling using simulation and cross-functional integration – Ubit Field Example. IPTC Paper 17163, presented at the International Petroleum technology Conference in Beijing, China, 26-28 March 2013.

Lee, H. J., Schwab, W. C., Edwards, B. D., Kayen, R. E., (1991). Quantitative controls on submarine slope failure morphology. Mar. Geotech.; v. 10; p. 143-157.

Lowe D. R., (1979). Sediment gravity flows: Their classification and some problems of application to natural flows and deposits. SEPM Special publication; v. 27; p. 75-82.

Mosher, D. C., Shipp, R. C., Moscardelli, L., Chayto, J. D., Baxter, C. D., Lee, H. J., Urgeles R., (eds.) (2010). Submarine mass movements and their consequences – 4th International Symposium. In: Advances in Natural and Technology Hazards Research, Springer, Dordrecht; v. 28; ISBN 978-90-481-3071-9.

Normak, W. R., and Gutmacher, C. E., (1988). Sur Submarine Slide, Monterey Fan, Central California. Sedimentology; v. 35; p. 629-647.

Onwude R. J., Jackson, C., Anidi, A., Ojo, A., Obere, F., Wanorue E., (2013). Maximizing recovery from gas injection in a complex channel system – Edop Field Case Study. SPE Paper 167592, presented at the Nigeria Annual International Conference and Exhibition held in Lagos, Nigeria, 30 July – 1 August 2013.

Reijers, T. J. A., Petters, S. W., and Nwajide, C. S., (1997). The Niger Delta Basin, in Selley, R.C., ed., African Basins – Sedimentary basin of the World 3: Amsterdam, Elsevier Science; p. 151-172.

Short, K. C., and Stauble, A. J., (1967). Outline of geology of the Niger Delta. American AAPG Bulletin; v. 51; p. 761-779.

Sternbach, C. A., (2018). Exploration creativity in the golden age of Super Basins - AAPG Initiatives: An african perspective. Search and Discovery Article 11167, adapted from oral presentation given at 2018 International Conference and Exhibition, Cape Town, South Africa, 4th November – 7th November, 2018.

Sumner, E. J., Talling, P. J., & Amy, L. A. (2009). Deposits of flows transitional between turbidity current and debris flow. Geology, v. 37; no. 11; p. 991-994. https://doi.org/10.1130/G30059A.1

Whiteman, A., (1982). Nigeria: Its Petroleum Geology, Resources and Potential: London, Graham and Trotman, 394 p.

NIGERIAN ASSOCIATION OF PETROLEUM EXPLORATIONISTS

SINCE 1975

# A Fit-for-Purpose Geological Evaluation Workflow for Non-Rig Well Work

**Omotayo-Johnson Mobolaji and Kuku Abimbola**
Chevron Nigeria Limited

## ABSTRACT

The depth of geological evaluation involved in non-rig well work (NRWW) can sometimes be under-documented as it tends to be more rigorous in the early phases of maturation of the opportunity. This paper seeks to highlight the geoscientist's role in non-rig well works by presenting a fit-for-purpose evaluation workflow developed in the maturing of five opportunities in the Western Niger Delta shelf. For a large field with over 140 existing wells, the evaluation can sometimes be very complex with conflicting well data. For a geoscientist, understanding spatial location of wells within the reservoirs and the implication of well performance on current reservoir condition are the most important task. In the reservoir of interest, the K-02, it was found that most of the shut-in wells had quit on low tubing head pressure indicating that the reservoir is pressure depleted. This might imply that few opportunities remain in the reservoir, given that this is a reservoir with a large gas cap and about 50% recovery. Pressure data from new drills through the reservoir however shows that the pressure in some fault compartments may be adequate to lift the oil to the surface. Based on geological evaluation, current reservoir conditions indicate that some of the shut-in wells were still within the reservoir oil band and still have the potential to flow simply by adding perforation above current interval. With the intent of using the gas cap as a potential gas lift, the perforation intervals were deliberately optimized to be as close to the current gas-oil contact as possible. Four perforation addition jobs in the reservoir and one zone switch opportunities into a shallower reservoir were proposed for execution. Two opportunities successfully executed led to significant production addition while others are still in different stages of maturation. A major challenge encountered is that with rapid pressure depletion, reservoirs with huge gas caps may ultimately have limited options of lifting oil to the surface, even with large remaining oil in place. Structural compartmentalization was also an issue as it limits how far dynamic fluid and pressure data can be extrapolated away from well control. An important lesson learned is that for a very big field with over a hundred wells, keeping an up-to-date well/reservoir status worksheet is recommended. This easily captures all well and reservoir information that will aid NRWW evaluation in one single repository.

**Keywords:** Geological, evaluation, Workflow, perforation, compartmentalization, reservoir, pressure, fluid contact.

## INTRODUCTION

Determining reservoir fluid contacts appears to be the single most important task in the NRWW process. Before the decision is made to zone switch out of the producing reservoir, it must be that the zone being abandoned is either gassed out or fully flushed. The intent of the evaluation is to determine whether the reservoirs have remaining economic accumulations and that wells are available to produce the opportunity. A new zone may then be selected that typically have good reservoir pressure and good potential and be structurally well placed within the reservoir (Bates *et al,* 2012). Additional perforation could be the recommendation if it is found that opportunities exist above current perforation in the same zone. From this effort, those wells that require a zone switch to shallower reservoirs are also determined. The evaluation also helps to verify if reservoir conditions favor any other well intervention such as gas lift, acid treatment or hot oiling before proposing any zone switch.

If zone switch is recommended, the same rigorous evaluation is carried out for the new reservoir of interest to ensure that the reservoir interval in the well falls within the oil band. The geological evaluation basically influences what type of well work – perforation addition, zone switch or other well intervention – to be recommended and determines the initial proposed perforation interval and how much hydrocarbon volume is being targeted.

### Reservoir Discussion

The K-02 is a saturated reservoir that has had significant



Sincere gratitude to the management of Chevron Nigeria Limited for the endorsement and support for this paper. The authors thank the leadership of the JV Asset Development in Chevron for their determination to continue to bring value. We would also like to thank all the internal reviewers for the feedbacks that helped improve the quality of the paper.
NAPE Bulletin, V.29 No 2 (November 2020) P. 8-12

production with peak production of in the 1980s. About thirty well have been completed in the reservoir to date (Figure 1). At the beginning of this study there were only two completions flowing from the reservoir. Material balance analysis indicates that the reservoir drive mechanism is a combination of gas cap expansion and water influx with little contribution from solution gas expansion. This is corroborated by the HGOR and HBSW seen in producing wells, depending on their placement on the structure.

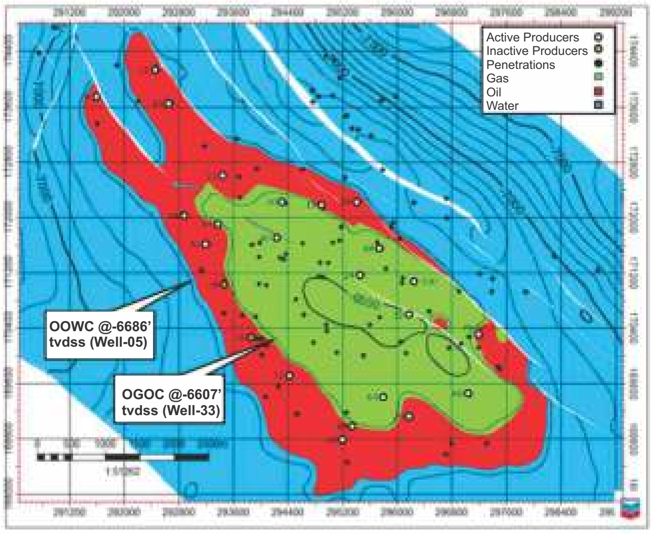


**Figure 1:** K-02 Original Fluid Distribution Map.

The reservoir was initially interpreted as a single flow unit within the hydrocarbon zone and the aquifer. Post-production wells data however revealed the development of differential oil-water contacts as identified by shallower contacts in two recently drilled well in the east of the reservoir than the production interval of the two producing wells in the west. Two distinct oil accumulations are believed to have been segregated due to crestal faulting and are most likely being depleted as separate tanks (Figure 2). The reservoir is however still connected in the aquifer hence the similarity in reservoir pressure across fault compartments.

The reservoir of interest, the K-02 is a saturated reservoir which was discovered in 1964 when the discovery well encountered 20 ft of net oil in the K-02 sand. The reservoir has currently produced 58.1% of its EUR. The reservoir exhibits a four-way faulted dip closure at the crest of the complexly faulted crested fault block (Figure 1). It has a large gas cap with a relatively small oil rim. About 81 wells have penetrated this reservoir to date. The original gas column is 144 ft, with an original oil column of 79 ft. The last recorded reservoir pressure is 1,708 psi representing about 43% decline from the initial recorded reservoir pressure of 2,934 psi in 1965. Most of the wells that produced from this reservoir quit on low tubing-head pressure (LTHP) due to extreme pressure depletion. The pressure challenge implies that even if opportunities still exist in some wells, getting enough pressure to push the oil to the tank appears to be a hinderance to successful execution of any well work.

## Reservoir Evaluation Workflow

In a complex field such as this with several producers at different points in the history of the field, a good starting point for geological evaluation is to develop a template that gives all reservoir and well information on a single database (Figure 3). A spreadsheet was developed that incorporated the status of all well strings in the reservoirs such as production status, current rate, water cut, existing non-rig well work plan and if plan is on current barge schedule, on the one hand, and the list of all available reservoirs penetrated by the well on the other.
The different sorting tabs includes:

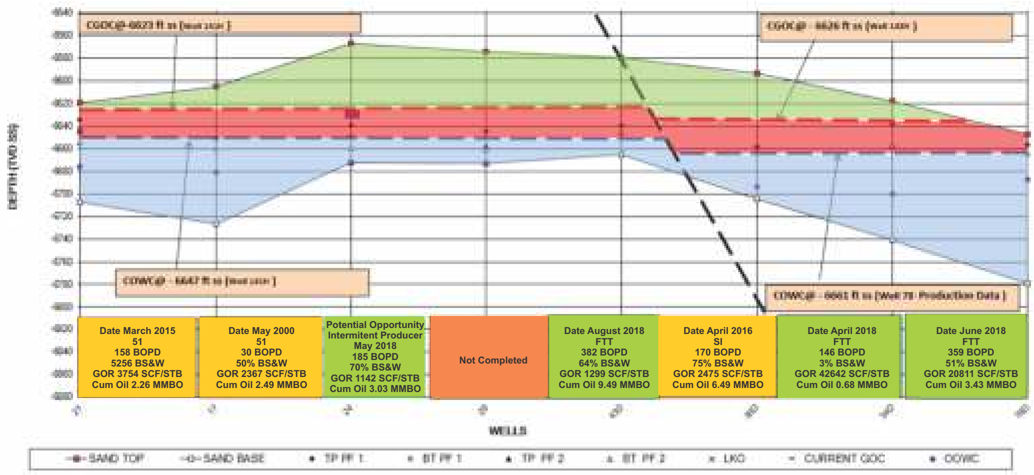


**Figure 2:** K-02 Reservoir Stick Diagram showing varying fluid contacts across crestal fault. Note that well 78 completed deeper is still producing while Wells 17 and 21 with shallower completions have quit.

1. Well status indicates whether well was flowing (ftt) or shut in for various reasons such as low tubing head pressure, high GOR, high water-cut etc.
2. Current production in barrels of oil per day (bopd): any well producing below a set economic limit can easily be identified.
3. Future plan column identifies wells that are already being progressed or matured to prevent duplication of effort.
4. Constrain tab indicates wells that have any sort of mechanical issues such as fish-in-hole, tubing issues, communication issues etc. that would prevent any immediate well work
5. BS&W indicates water cut and give an idea of possibility for gas-lift as an option
6. List of Reservoirs penetrated by each well string, color coded according to the fluid type encountered (gas, oil or water). Also indicated is the oil and gas column encountered. The current producer can be uniquely color-coded to easily show which are the remaining potential candidate for zone switch to shallower reservoirs.

With this database in place, it was easy to sort by wells that have been shut in and for what reason they were shut in as well as wells that were flowing. Wells that had very low production volume can also be identified early on as future opportunities so that the queue of opportunities is updated for timely interventions. \

This might be a tedious exercise for a field with over 200 well strings and will need to be constantly updated to keep well status up-to-date, but the front-end loading exercise provides an evergreen resource that churns out potential well work opportunities and helps focus the geologist's attention on reservoirs of interest.

In this case, sorting through well status on the field database revealed that the K-02 reservoir had a good number of wells that were shut in on low tubing head pressure even at relatively low water cut. Nodal analysis was carried out and excludes the option of gas lift to sustain and optimize flow in many of these wells.

Next phase was the actual geological evaluation of the reservoir to understand why wells in the reservoir had this unique status. Fluid contact evaluation showed the reservoir still had between 24-40ft of oil in place. Four new wells drilled in 2016 revealed that while Gas-Oil contacts variation was not significant, Oil-Water contacts varied by up to 20ft across the faults. For the eastern flank, current OWC is from one of the wells was -6,647' tvdss and an OUT at- 6623ft. TVDSS. On the western side, another new well encountered an ODT at 6656 ft tvdss and is corroborated by material balance (2018) which puts the COWC in the western flank at 6659ft tvdss.

Along with saturation logs, production data and material balance analysis were also used to estimate fluid contacts for comparison. Contact estimation from water cut information assumes that the percentage of water-cut corresponds to the fraction of the perforation interval covered by water. Water cut could however be affected by coning and could vary significantly in case of a slanting contact. It should be noted that production-based oil-water contacts tend to be more pessimistic than the reality. Formation water is believed to move faster than oil in a bottom water reservoir especially where withdrawal rate is high (Tu *et al,* 2007).

The challenge to production from the reservoir was the magnitude of pressure depletion that meant that even though there was still up to 60mmbo in place volume in the

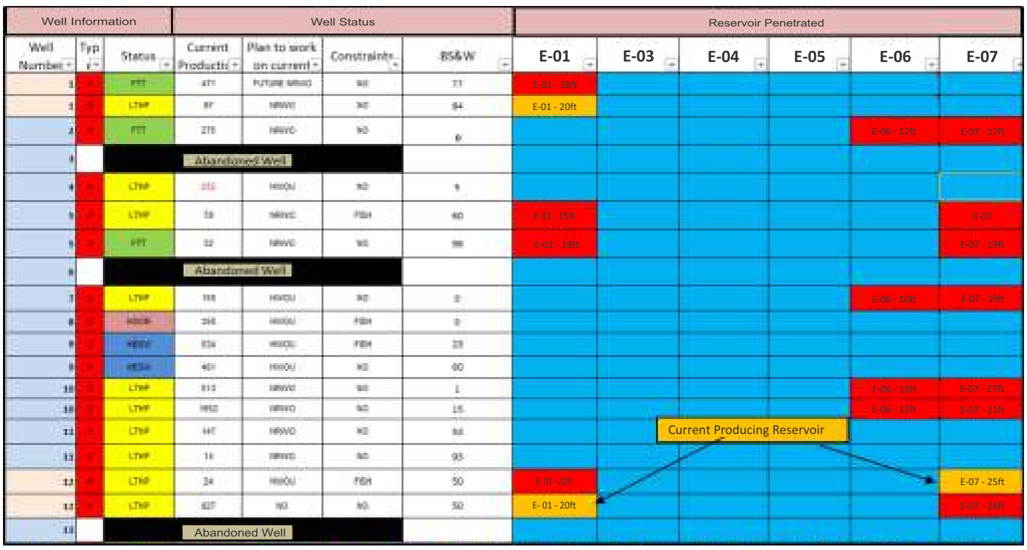


**Figure 3:** Non-Rig Work Over Geological Evaluation Data Sheet with well and reservoir information. Database allows integration of all required NRWO information for effortless evaluation.

reservoir, most of this volume could not be brought to the surface. Some of the wells however revealed suspected partial dynamic pressure compartmentalization due to the complex system of crestal collapse faults. It appears that some fault blocks were able to act as partially closed systems with possible lower decline rates with high enough pressure to sustain fluid flow for longer. Several of the wells that had quit were found to still have perforation interval within the oil band encountered in the new drills. The reservoir has a huge gas cap and simply adding perforation at an optimized interval close to the gas cap could be used to lighten the tubing column somewhat to get the oil to the surface. These wells were proposed for additional perforation above existing intervals (Figure 4).

responsible for shallower fluid contacts and higher-pressure depletion. When production from this side stopped, it appears the zone had had chance to re-equilibrate baffled, as it were, from the rest of the pool by the fault where production was still ongoing. Wells that had perforation interval still within the oil band in these fault blocks were identified and flow-tested. One of such wells, well 24 came back onstream with about 200bopd production. Other wells in these fault blocks were evaluated for potential perforation addition well work and wells 17, 21, 24 and 36 were thus identified.

Choice of perforation interval is another task the geologist must undertake. Usually the perforation interval would

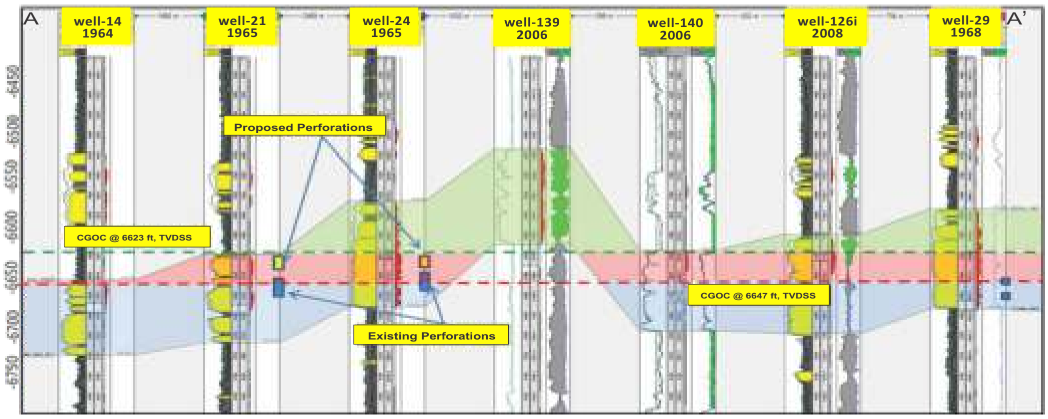


**Figure 4:** K-02 Structural Cross-section Showing Current Fluid Contacts. Identified perforation addition opportunities are indicated in yellow box

Pressure data taken from some of the new wells revealed that fault compartments do exist with significantly higher pressure that could get the oil to the tank. It was found that withdrawal rate had been higher in the eastern more faulted area at the earlier phase of production and this was

need a compromise with the asset Engineer to be as far from the gas and water as possible but in the K-02 reservoir, the choice was to be close to the GOC to enable some gas into the tubing to lighten the fluid as a form of gas lift mechanism. Water Cut Sensitivity Analysis for well 24

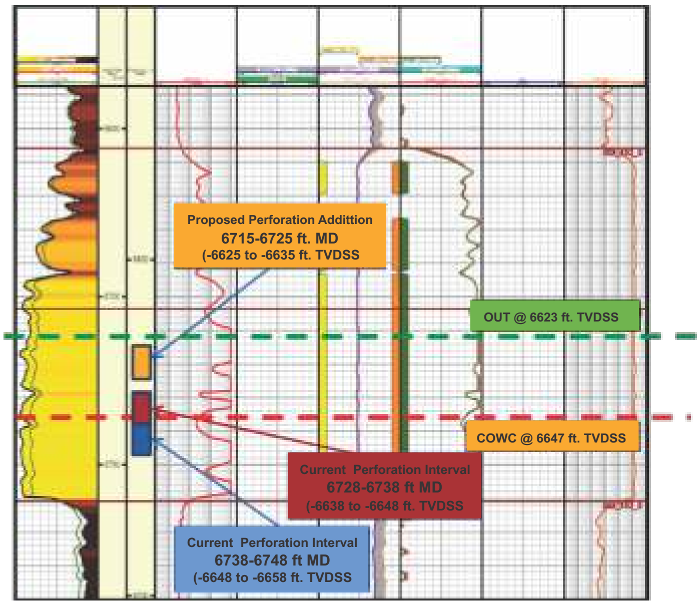


**Figure 5:** Well 24 Well Log showing Proposed Perforation Addition.

indicates that the reservoir pressure would be able to sustain flow naturally to a water cut of 76% while the well was already at over 70% water cut. The wells were therefore going to need gas lift to continue producing. Getting the optimal perforation interval was important to the expected production increase as the this would determine extended life of the additional production.

## DISCUSSION AND CONCLUSION

The last measured reservoir pressure from a well within the viable fault block was 1,718 psi (June 2016) representing about 43% decline from the initial recorded reservoir pressure of 2,934 psi in 1965. This is significantly higher than the 1250 psi that was recorded before this as part of well surveillance from areas with higher pressure depletion rate

Production add of up to 67% increase on the old rate was recorded in well 24 by adding perforation at an optimal interval within the oil band above current perforation indicating that even in this highly depleted, pressure challenged reservoirs, non-rig well work could still salvage some value. Other opportunities are being matured leveraging the lessons learned from the well 24 well work result. (Figure 5).

An important challenge with this reservoir is that with rapid pressure depletion, reservoirs with huge gas caps may ultimately have limited options of lifting oil to the surface, even with large remaining oil in place. This reservoir had many take points at a time and voidage replacement was not going on. One thing that could have helped was to be more conservative in production rates so that the reservoir gets the change to significantly maintain its pressure.

While extrapolating reservoir properties as seen in wells, structural compartmentalization severely limits how far fluid and pressure data can be extrapolated away from well control This often means we do not know if a well is going to behave a certain way or not. In terms of best practices, for a very big field with over a hundred wells, keeping a well/reservoir status worksheet is recommended. This easily captures all well and reservoir information that will aid NRWO evaluation. Well production data needs to be integrated in this database with pressure data and dynamic reservoir characterization to fully assess an opportunity.

An important lesson learned is that teams should be willing to exhaust all available options in producing from a zone before considering zone switching to another. Sometimes with significant pressure depletion, some seemingly viable geological opportunity may not be technically possible to mature.

## REFERENCES CITED

Bates, G., Bagoo, D., Garcia, D., Finol, A., Nazarov, R., Rivas, C., … Bunraj, C. (2012, January 1). Production Optimization of a Mature Offshore Asset. Society of Petroleum Engineers.

Tu, X., Peng, D. L., & Chen, Z. (2007, January 1). Research and Field Application Of Water Coning Control With Production Balanced Method In Bottom-Water Reservoir. Society of Petroleum Engineers.

NIGERIAN ASSOCIATION OF PETROLEUM EXPLORATIONISTS

SINCE 1975

# First De-Ghost Depth Migrated 4D Signal on Akpo Field: From Acquisition to Innovative Processing Adaptations and Impact

[1]A. Adeyemi; [2]M. Esotu*; [3]M. Erbetta; [4]E. Ogu; [5]R. Salami and [6]P. G. Smith
[1,2,3,4,5]Total E & P and [6]Bulwark-ION

## ABSTRACT

For close to a decade, seismic monitoring campaigns over the Akpo Field have been quite successful in impacting infill well development and reservoir management decisions. In 2018, a dedicated low-cost seismic monitor survey was acquired while achieving high repeatability metrics (lower dS+dR) in both the obstructed and the non-obstructed parts of the field. This was made possible with real-time iterative fold and repeatability acquisition QCs between vessel offshore and onshore site. Prior to 2018, 4D seismic has been utilized rather qualitatively relying on narrow bandwidth time-migrated 4D signal. With the 2018 survey, a 4D seismic processing flow was innovatively adapted to de-ghost the 4D signal after the main de-multiple flow and then depth-migrate the 4D signal using a prior TTI PSDM velocity model after just one update of tomography. The combined results of the carefully executed 4D seismic acquisition survey and specialized non-conventional processing techniques has resulted in the first ever de-ghosted, larger bandwidth, depth-migrated 4D signal on the Akpo Field. Initial results show that the 4D signal thus obtained is better resolved, more coherent with geology and more laterally continuous. This has increased confidence in the robustness of the 4D seismic in impacting infill drilling as well as permitting a more quantitative use of the 4D signal for model history-matching and dynamic model update for better forecasting of remaining field reserves in the maturing field. Akpo field is operated by Total Upstream Nigeria Limited (TUPNI) on behalf of NNPC, SAPETRO, PETROBRAS and CNOOC.

**Keywords:** De-ghosting, migration, seismic, processing, velocity, tomography, 3D regularization, amplitude, destripping, modelling.

## INTRODUCTION

The Akpo field, operated by TUPNI, is located deep offshore, Nigeria and is 200km south of Port-Harcourt. The water depth varies from 1200m to 1500m and the reservoirs are turbidite channel complexes and lobes of Miocene age, containing under saturated critical fluids. Figure 1 shows the location of Akpo field relative to other big fields in the Niger Delta basin.

Since the first oil in 2009, previous monitor surveys acquired include Monitor 1 (M1) in 2011, Monitor 2 (M2) in 2015 and the very recent Monitor 3 (M3) in 2018. The baseline seismic was acquired in 1998 while the undershoot baseline seismic was acquired in 2009 covering the area with fixed surface installations (Akpo FPSO & Offloading Buoy).

After 10 years of production, the Akpo field has recorded great successes with 4D monitor surveys. For example, the M2 facilitated the identification of un-swept areas leading to infill drilling opportunities (Adeyemi et al , 2018). The M3 processing was in two phases, the fast track and the full processing, the full processing of the M3 was carried out using a de-ghosted depth migrated approach, with the aim of pushing the fast track volumes (which was a 4D conventional PSTM delivered four months after the last shot point of the M3 2018 acquisition) to yield better results.

With these additional processing steps included, we were able to:

- Achieve bandwidth extension targeted at improving the low frequencies and enabling sharper and more continuous 4D signal;
- Increasing the 4D signal to noise ratio;
- Improving the lateral positioning and focusing of the 4D signal with one pass of velocity update and;
- Optimize the global matching between the three monitors, which was one of the feedbacks from the inversion team, in order to get better results from the 4D inversion.

## OBJECTIVES & CHALLENGES

The main geophysical challenge was to use an optimized workflow to extract a sharp and accurate 4D signature with a minimal turnaround time. The asset objectives of



The authors would like to thank the OML 130 partners – NNPC, SAPETRO, PETROBRAS, CNOOC and TOTAL for their permission to publish and present this paper. Special thanks also to Bulwark-ION for processing this data in record time with good quality output, and the entire geophysics operations and Total Akpo-GSR teams for their support.
NAPE Bulletin, V.29 No 2 (November 2020) P. 13-19

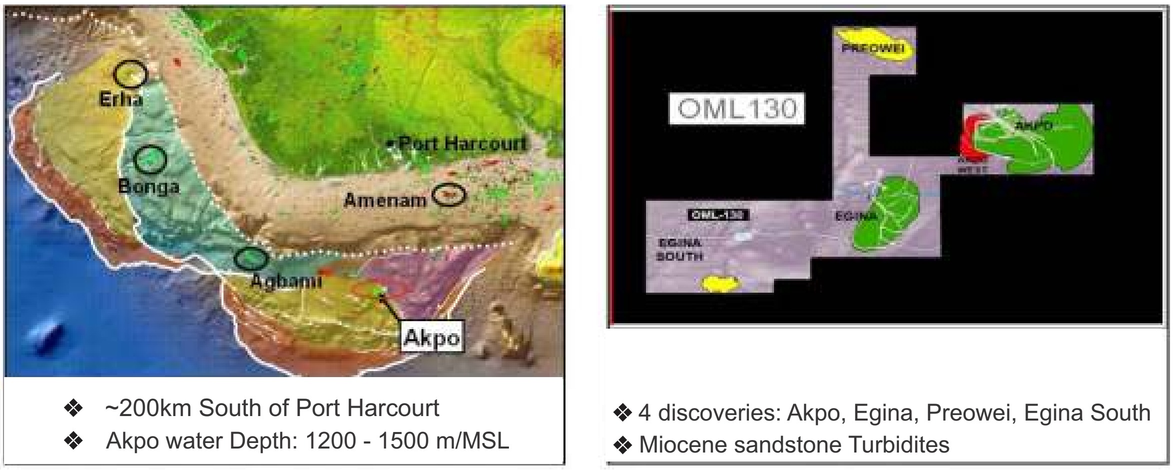


**Figure 1:** Regional location of Akpo field.

the 4D seismic were for reservoir monitoring & management; identifying infill opportunities, bypassed zones and as a guide for potential well intervention.

**Increased Repeatability in Acquisition**

In 4D processing, to detect changes in the reservoir, good repeatability of acquisition parameters is key to achieving good 4D results. However, getting the right match between surveys can be challenging given that the circumstances surrounding the previous acquisition will differ, with changes in factors such as ocean currents, temperature, tides and surface obstructions on the field. To mitigate this, it is highly recommended to have steerable streamers (to maintain source tracks and streamers on pre-plot), and also to have real time current data and a 4D in-field acquisition specialist onboard for optimal line planning. In order to reduce the impact of the listed factors, infills are designed and acquired so as to improve on 4D repeatability in areas of low fold. The baseline and the monitor surveys on Akpo field, apart from M1, involved single and dual vessel operations. The constraints of the fixed surface obstructions, Akpo FPSO & Offloading Buoy with about 2 km of separation between them as shown in Figure 2, led to an innovative design, which is the use of a push-pull asymmetric streamer configuration which enabled the acquisition of the 5200m far offset with reduced number of streamers and streamer length (the initial recording spread is therefore roughly divided by four due to HSE related risk in the obstructed area). This acquisition technique was used for the first time on Akpo field and in Nigeria in 2009.

The single vessel operation consisted of a spread of 8 streamers, each of 5200 m length and separated by 100 m, while the dual vessel operation consisted of four streamers, each of 2600m length and separated by 100m. In order to acquire the same offsets range and CDP lines comparable to the single vessel mode, it is necessary to navigate four times (two times in push and two times in pull) to acquire same data. The pull mode involves the source vessel leading the streamer vessel by 2600m for acquisition of long offsets (from 2600 to 5200m) while the push mode involves the source vessel lagging the streamer vessel by 350m for acquisition of the short offsets (from 350 to 2600m). The undershoot of the FPSO and the

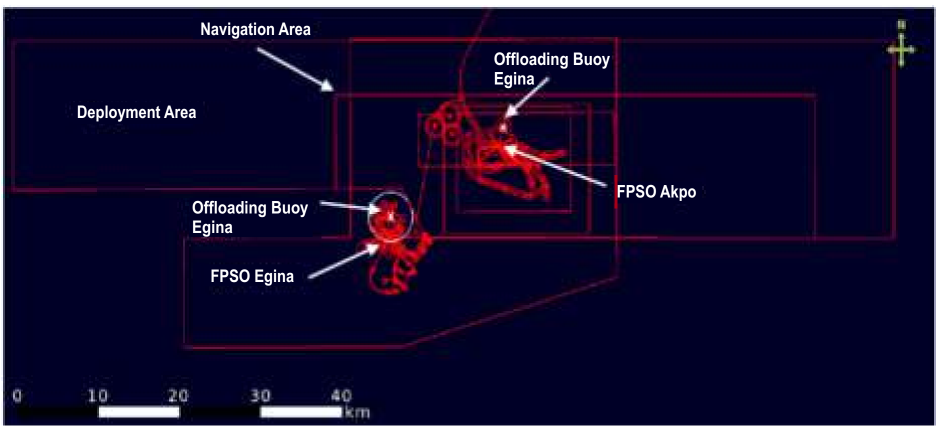


**Figure 2:** Survey Layout and Obstructions.

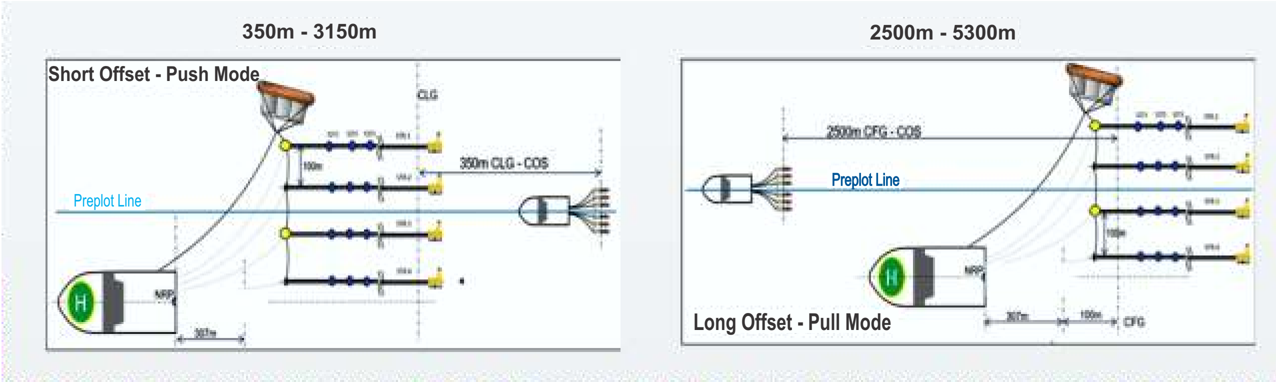


**Figure 3:** Configuration showing Dual Vessel configurations during Akpo 4DM3. Long offset – Pull Mode (Right) and the Short offset – Push mode (Left)

offloading buoy, and acquisition of the lines in between the obstructions (Figure 2), are facilitated using this acquisition push-pull method (Figure 3).

For the M3 acquisition, the pre-plot was the post-plot of M2 (prime & infill lines) with slight smoothening. Steerable streamers, near real time current data and optimal line planning by a 4D in-field acquisition specialist aided in obtaining very good dataset with medium to high level of 4D repeatability and coverage

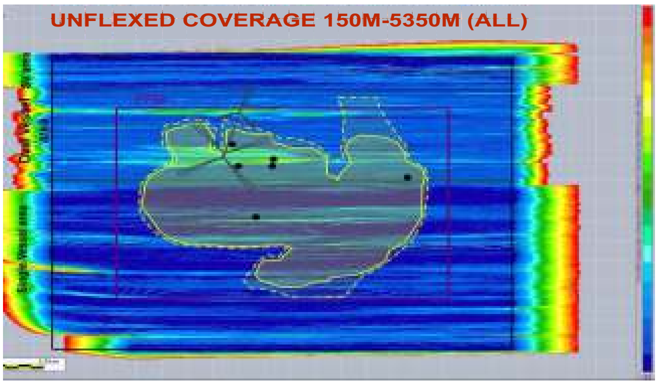


**Figure 4:** Unflexed coverage (150m – 5350m). Full fold achieved in both the single and dual vessel areas.

(Figures 4 and 5). There was an additional constraint on the SW part of the survey area – the Egina OLT Buoy installation where 3 km exclusion zone was agreed. This affected the Run-in & Run-out in that area and consequently, the coverage without any detrimental impact on 4D signal at the reservoir level. There was a significant cost savings on the M3 survey due to better management, optimization and contractual conditions than for M2 in 2015. Lastly, the survey was completed safely without any significant or high potential HSE or Security incident and this was achieved in record time.

## 4D Processing

The 4D processing was done in two phases, the anisotropic PSTM fast track (delivered four months after the last shot-point), and the anisotropic PSDM full processing delivered six months later. The processing workflow was designed to co-process all three vintages together (Table 1), with M2 serving as the reference survey in those two separate instances. The fast track of the M3 used the regular 4D processing scope, while the full processing had additional processes such as de-ghosting and imaging, which were done for the first time on the Akpo field. Noteworthy is the fact that, the lessons learned during the fast track processing particularly for

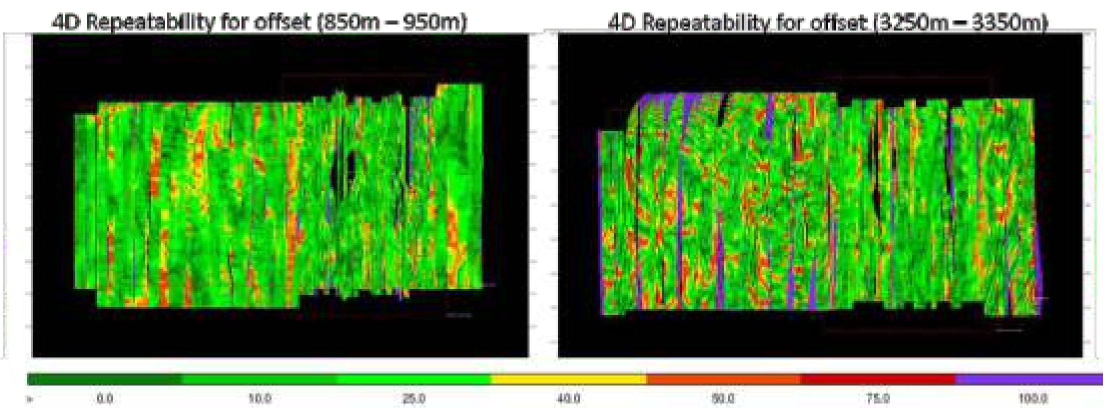


**Figure 5:** 4D Repeatability for Near and Far Offset.

statics, matching, demultiple, destripping, 4D binning and regularization, were valuably used to optimize the full processing.
In a bid to achieve a good 4D signal, it was necessary to reduce the 4D background noise seen in the fast track. Therefore, multiple passes of denoise were applied in different domains on the co-processing of the three surveys to optimize the results. This can be seen in the 4D RMS and NRMS maps shown comparing results of the fast track and the full processing. The process of matching covered the overburden section, within the reservoir area and also in deeper sections. It was possible to closely monitor the progress of the processing with milestone 4D QCs carried out at intervals after major processing steps. Table 1 below shows the processing sequence applied to the full processing, text in red are the additional processes applied for the first time on the Akpo Field.

**De-ghosting:**
Conventional towed marine streamer suffers from sea surface ghost reflections, thereby compromising on signal bandwidth and limiting the resolution of seismic events and attenuation of deep signals. This can be seen as notches in the amplitude spectra as shown in Figure 6, corresponding to source and streamer depths at 5m and 8m respectively. A de-ghosting technique was used to address the above issue caused by surface ghost in order to increase the bandwidth of the data. Broadband data are well suited for 4D reservoir monitoring, for optimized recovery and decrease the interpretation uncertainty at reservoir level. Additionally, this rich low frequency solution enables accurate inversion of data, better structural & stratigraphic definitions, improved lithology, fluid prediction and serves as an optimal guide in making drilling decisions (Agnisola *et al.,* 2018).

Low frequencies are less impacted from earth's attenuation effects and can penetrate deeper layers. Low frequency data are also beneficial for waveform and impedance inversion as richness in low frequencies allows for better constraints in inversion results. The process of deghosting will ultimately boost both the low and high frequencies as it fills in the amplitude spectra around the notch frequency locations.

It was also necessary to apply several passes of denoise in multiple domains, each handling different noise elements, both random and linear (Hicks *et al.,* 2014). However, for the full processing sequence, it was decided that the 3D Surface Related Multiple Elimination (SRME) de-multiple output from the fast track, will be a good starting point for the full processing, as this route will minimize the impact of the boosted residual noise after deghosting. The already zero phased data was converted back to minimum phase to adhere to the deghosting assumption of an input minimum phase wavelet. Further testing ensured neither ringing nor artefacts were introduced post application of the deghosting process. Figure 7 shows results of de-ghosting in pre-stack domain showing a boost in low frequency.

**Table 1:** Processing Sequence of Full processing Sequence (red text signifies the first time processes applied on the Akpo Field)

| |
|---|
| INPUT NAV DATA - DESIGNATURE - DENOISE - DEMULTIPLE - AMPLITUDE DESTRIPPING - RMC - AMPLITUDE DESTRIPPING - INITIAL GLOBAL MATCHING - COLD WATER STATICS |
| 3D SRME - DENOISE - DEGHOSTING - RESIDUAL DEBUBBLE - Q - PHASE ONLY |
| GLOBAL FOOTPRINT REMOVAL - FREQUENCY MATCHING |
| RESIDUAL 4D TIME & AMPLITUDE DESTRIPPING - 4D BINNING - 3D REGULARIZATION |
| RADON DEMULTIPLE - RESIDUAL DENOISE (OFFSET) - VELOCITY MODEL BUILDING (1 UPDATE) |
| TTI KPRESDM - RMO CORRECTION - STACK - Q - AMPLITUDE ONLY - 3D FXY DECONVOLUTION |
| FREQUENCY MATCHING - TIME & AMPLITUDE DESTRIPPING |

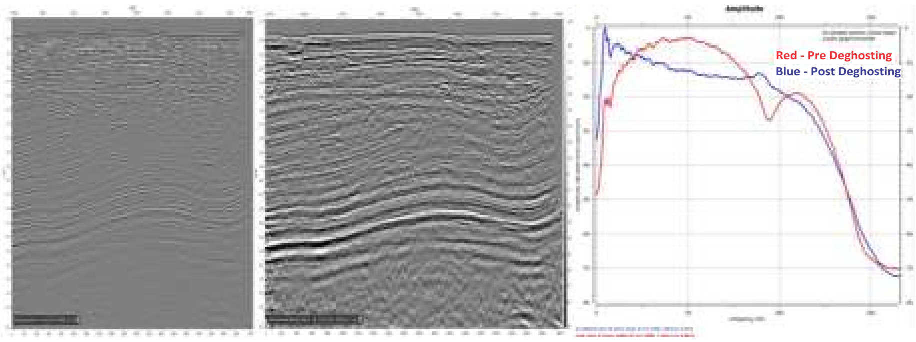


**Figure 6:** 2D Stack pre-deghosting (left) and post de-ghosting (middle). Amplitude spectra (right); red spectra (pre-deghosting) and blue spectra (post-deghosting).

**Velocity Model Building**

In 2011, a depth velocity model was built for the Akpo field using the baseline data. This has been the reference velocity model for well placements. During the full processing of the M3, this model was updated to improve

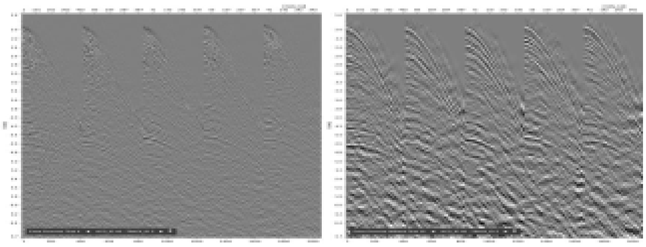

**Figure 7:** 2D gathers before (left) and after (right) Deghosting.

spatial positioning of structures and focusing of 4D signals. Using the newly de-ghosted datasets, one pass of velocity model update was performed, using conventional tomography in order to achieve a better stack response thus leading to sharper structural continuity of the 4D signatures, delineating flushed zones from bypassed zones.

The baseline data was selected for the tomography process. To ensure a stable automatic picking was achieved, the data was pre-conditioned in the XT domain. Gathers on a 50m x 50m grid were muted at 45 degrees to remove far offset stretch. Further cleaning of the gathers included attenuating the steeply dipping aliased multiple and eliminating high frequency noise which can interfere with the automatic picking and gridded tomography iteration process. One pass of long wavelength (800mx800mx240m) tomography was carried out to resolve the velocity variations seen in the initial (2011) model.

Depth misties analysis was done after the tomography velocity update by comparing well depth markers with seismic events. Several target lines were migrated to ensure structural consistency and that 4D effects are properly imaged. Improved gather flatness and structurally aligned signal coherency on the QC target lines indicated that the velocity model update was successful. Figure 8 shows comparison of the new velocity model and the initial model, with the DV (difference in velocity) derived from the new and the old models.

Furthermore, due to the poor picks observed in the deeper section, a horizon was used to constrain the picks in the deep units to avoid introducing artefacts into the model. After tomography inversion, a delta update was applied to maintain gather flatness and marker positions at the original depths. Depth misties carried out by the asset interpretation team on this data showed great improvement compared to misties derived from the 2011 velocity model. The improved velocity model was used for the final pre-stack depth migration on all three surveys.

**RESULTS**

After the full processing, a significant impact on the qualitative and quantitative interpretation was achieved thanks to this new 4D processing approach including the addition of the de-ghosting and an update of the velocity model, needed to run an anisotropic pre-stack depth migration (PSDM). With the extra denoise steps applied in various domains, a major reduction in the 4D background noise was observed. Destripping and statics correction steps aided the convergence of time shifts (between the Base98 and M3 surveys) to the reference M2 survey, which in turn reduced the acquisition footprints and improved clarity of the 4D effects. Global matching done pre stack and post stack reduced the effects of residual 4D differences between survey pairs.

4D co-binning, using small ds+dr (repeatability between surveys) pairs between the three surveys made significant improvement with regards to the 4D NRMS (which measures the sensitivity of the repeatability metrics, with regards to the signal time shift and the signal bandwidth). It was also discovered that by limiting the ds+dr, we were

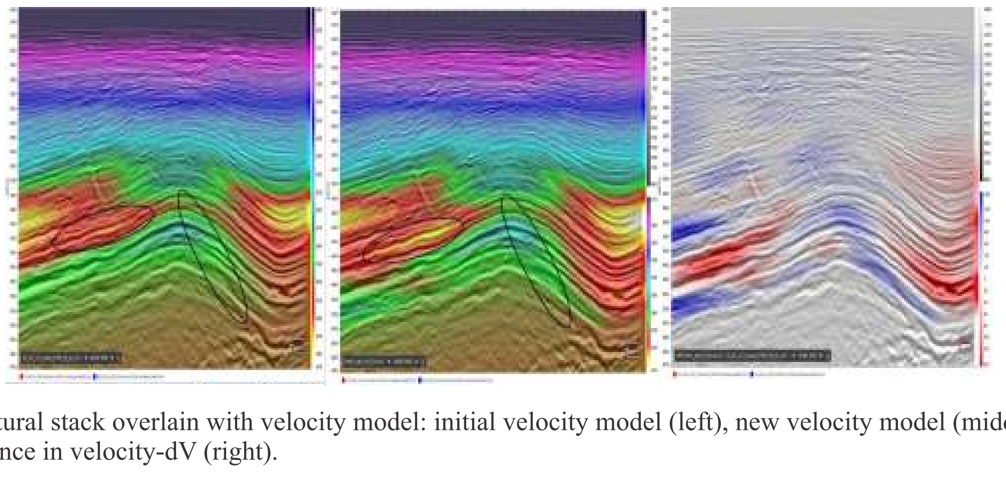

**Figure 8:** Structural stack overlain with velocity model: initial velocity model (left), new velocity model (middle), difference in velocity-dV (right).

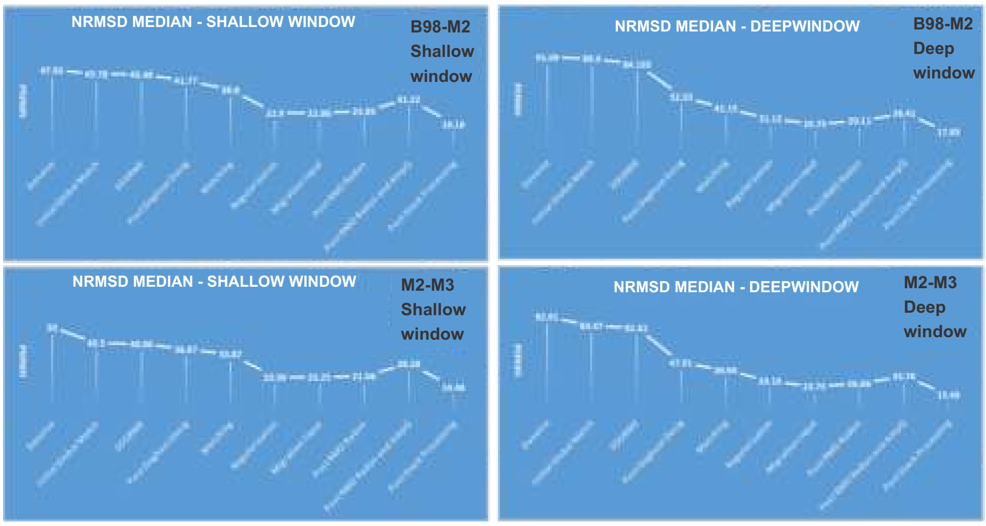


**Figure 9:** 4D NRMS evolution from the initial denoise to the final post stack processes applied to the data.

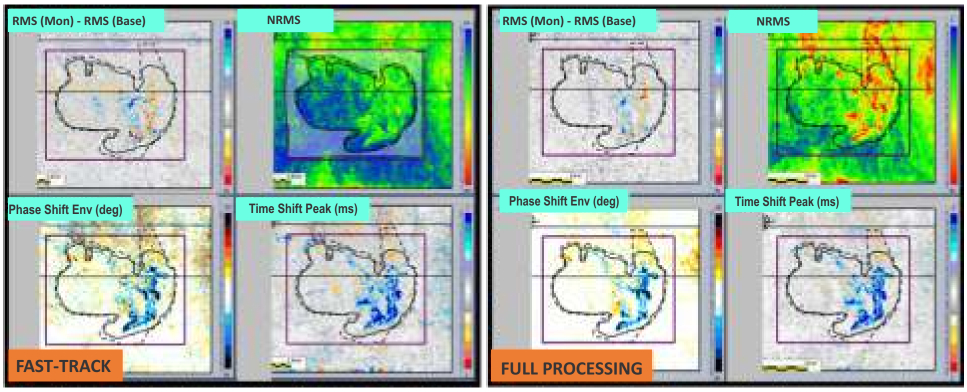


**Figure 10:** : Qualitative differences between the FAST TRACK and FULL PROCESSING sequences in the major producing interval where activity is at its peak. *(Note the differences in scale between the fast track NRMS (10-130) and the full processing NRMS (5-60) (Burren & Lecerf, 2014))..*

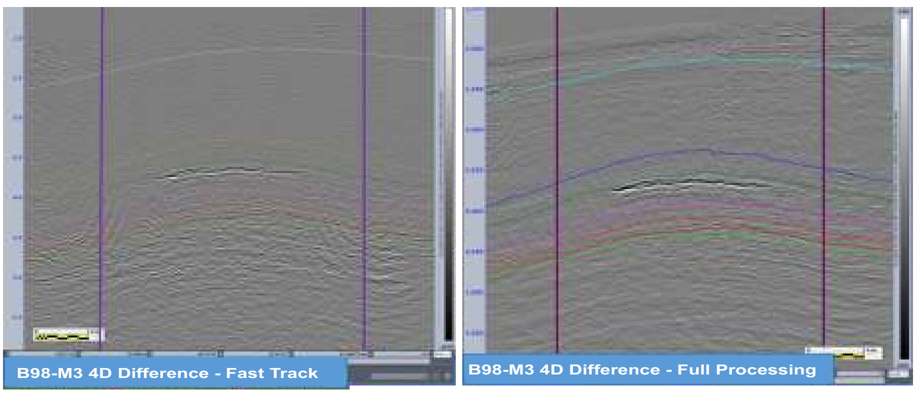


**Figure 11:** 4D difference of a crossline section across the Akpo field. Horizons overlaid represent overburden (between 2.5 – 3.5secs) and producing reservoirs (between 4.0 – 4.8secs). This depicts the difference seen between the anisotropic PSTM fast track on the left and the anisotropic PSDM full processing on the right. Less 4D noise on the full processing and there is better resolution. *(Note there are gain functions and scaling differences due to amplitude Q applied to the full processing).*

able to eliminate the migration noise (feedback from fast track processing). The co-binned traces were fed into a regularization process, where small holes and empty bins (<250m) were filled, which helped to reduce migration artefacts that can arise from missing data and minimize acquisition footprints seen on the maps. Figure 9 shows a summary of the 4D NRMS progress tracked with 4D milestone QC's during the co-processing of all three

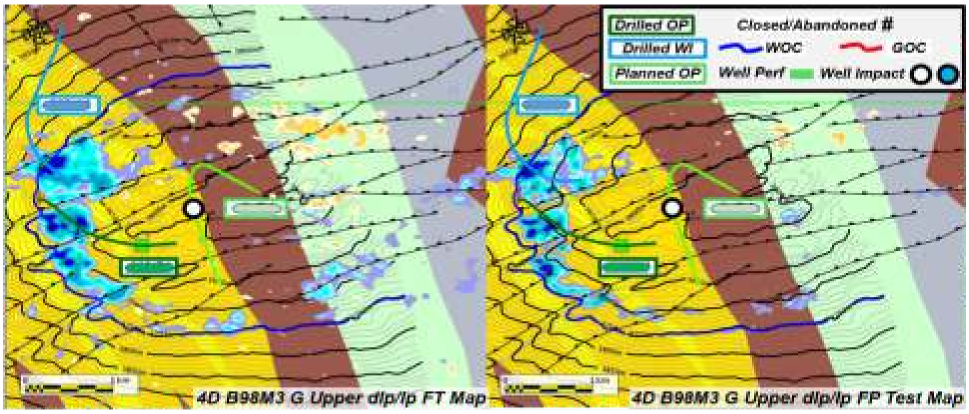


**Figure 12:** Comparison between the Fast track (left) and full Processing (right), maps extracted are from one of the deeper reservoir levels overlain with 4D "change in impedance" between B98 and M3 over a period of 10 years.

surveys.
An anisotropic Pre-stack depth migration was run for all three surveys. This brought about further improved spatial positioning of the structures and increased focusing for more precise 4D differences. From the results below, a better focusing within the reservoir zone and better delineation of the fault structures is seen in the Akpo field. Figures 10 and 11 respectively shows maps and sections that cut across the producing reservoirs, with improvements achieved between the fast track and the full processing.

## IMPACT

Preliminary results from 4D inversion, seen on the change in impedance, show that the fast track and the full processing have visible differences. The full processing shows better focusing and cleaner 4D signals. On the fast track, it appears what the asset thought was an over pressured zone (patches of orange) in the north east has drastically reduced (Figure 12). The obvious water anomalies seen in the west are similar, what we see as blurry in the fast track has sharper details in the full processing. Therefore, we have improved the illumination of this particular reservoir, as we see the 4D inversion gives more stable results permitting a more quantitative use of the 4D seismic data for history matching and dynamic model update, as well as confirming the location of infill wells on Akpo field.

## CONCLUSION

Real time follow up of Akpo field 4D seismic acquisition and the use of steerable streamers helped to increase the much needed repeatability for a successful 4D seismic acquisition. Overall, good repeatability (ds+dr) was achieved between the M2 and the M3 even in areas with surface obstructions.

The Akpo 4D M3 processing followed two routes, the fast track processing and the full processing. For both processing routes, all three vintages B98, M2 (2015), M3 (2018) and their corresponding undershoots were co-processed together. The full processing had extra processes in the work flow such as optimizing the denoise, applying de-ghosting for bandwidth expansions and depth imaging, which was the first time for the field. With these steps, a major success has been achieved in the processing results seen on the full processing.

The velocity model update improved gather flatness and are more structurally coherent with the seismic image, most especially on the flanks. The results have confirmed with certainty that the addition of these processing steps have increased confidence in the robustness of the 4D seismic and have positively impacted infill drilling program.

## REFERENCES CITED

A. Adeyemi, T. Tyagi, V. Biu, G. Uweriokwe, P. Wantong, H. Atoyebi, J. Oukmal, J. Aiyemobola, L. Nosike, V. Onwuchekwa and M. Usman (2018). Value of 4D-Seismic in Field Development Drilling and Minimizing well interventions in a maturing deep offshore turbidite field. NAPE 36th International Conference and Exhibition, November 2018, Lagos, Nigeria.

E. Hicks, H. Hoeber, G. Poole, B King (2014). An Efficient 4D Processing Flow of Variable-Depth Streamer Data. The Leading Edge. Volume 33 Issue 2, February 2014,Pages: 105–220ISSN (print):1070-485X ISSN (online):1938-3789

J. Burren & D. Lecerf (2014). Repeatability Measure for Broadband 4D seismic. Conference Proceedings, Second EAGE/SBGF Workshop 2014, Nov 2014, cp-435-00016 ISBN 978-94-6282

Johnston, D. H (2013). Practical applications of time-lapse seismic data; Society of Exploration Geophysicists, 2013 Distinguished Instructor Short Course Distinguished Instructor Series, No. 16 ISBN 978-1-56080-086-6 (Series), ISBN 978-1-56080-307-2 (Volume) pp. 73 -81

P. Agnisola, R. O'Driscoll, P. Smith, D. Chu, E. Assiak, C. Ugwuez3e and P, Ukerun (2018). The Effect of Deghosting on the 4D Response: Usan Field, Nigeria. 80th EAGE Conference and Exhibition June 11-14 2018 Copenhagen, Denmark

NIGERIAN ASSOCIATION OF PETROLEUM EXPLORATIONISTS

SINCE 1975

# Opportunity Generation in Mature Field Settings using Spectral Decomposition: Niger Delta Field Examples

**Amidu S. A.*, Obere F. O., Agbegha E., Akinpelu J. K., Medema G. F., Ochogbu P. I. and Salisu A.**
Mobil Producing Nigeria Unlimited, Lagos Nigeria

**ABSTRACT**

The current operating environment, arising from volatile oil prices, challenges the industry to be proactive with cost saving innovations and application of cutting-edge technology. Spectral decomposition technology (SDT) is a proven method for enhancing opportunity generation and optimizing well placement through better imaging of subtle structural and stratigraphic features. Three case studies of SDT integration for drill well opportunity generation in mature field settings offshore Niger Delta are presented. In all cases, SDT allowed us to discriminate the most significant frequency components and optimize seismic data for structural and stratigraphic interpretation. Deepwater examples are taken from two fields where SDT was used to delineate thin-beds that fall at or below seismic resolution. SDT enhanced stratigraphic details that were not obvious in traditional amplitude extractions. Results were used for improved Environment of Deposition (EOD) definition, reservoir connectivity and well placement optimization. In the shallow water environment example, SDT was used to enhance regional mapping of fluid contacts (flat events) in a shallow water field. Frequency volumes aided mapping of gas-oil-contact (GOC) and oil-water-contact (OWC) at locations where they were less visible on traditional stacked time-domain seismic volumes. Results were successfully used as part of field-wide review to assess future opportunities in the field. In some of the cases, additional deeper and shallower anomalies were identified, which could be subjects of future investigations. The technology is currently being used to support other ongoing projects in shallow JV and Deepwater fields.

**Keywords:** Spectral, decomposition, seismic, amplitude, extraction, frequency, deepwater, gas-oil-contact, oil-water-contact.

## INTRODUCTION

SDT is an important analysis tool that is used to decompose seismic signal into its constituent frequencies. This allows the interpreter to see amplitude and phase tuned to specific wavelengths, just as a radio can pick out a single station, or prism a single color (Hall and Trouillot, 2004). SDT decomposes the seismic data into individual frequency components that fall within the measured seismic bandwidth, so that the same subsurface can be viewed at different frequencies (Partyka *et al.,* 1999). Because stratigraphy resonates at wavelengths dependent on the bedding thickness, thin beds or features will be tuned and have relatively higher amplitude at higher frequencies (McArdle and Ackers, 2012).

SDT has been employed in seismic interpretation over the past decades and has become a well-established tool that helps in the analysis of subtle structural and stratigraphic features. Partyka *et al.,* (1999) introduced SDT as an interpretation technique and presented an interpretation workflow that was successfully used for imaging and mapping of temporal bed thickness and geologic discontinuities in 3D seismic data. Since then, spectral decomposition has been widely used in seismic data interpretation in applications such as stratigraphic and complex fault system characterization (Marforth and Kirlin, 2001; Wei, 2010), quantitative reservoir characterization (Hall and Trouillot, 2004; McArdle and Ackers, 2012), gas identification (Burnett *et al.,* 2003; Odebeatu et al., 2006), and direct hydrocarbon detection (Yoon and Farfour, 2012). In all cases, SDT is shown to be a robust tool to enhance structural and stratigraphic interpretation.

In this paper, we present three case studies of SDT integration for opportunity generation in mature field settings offshore Niger Delta. In all cases, SDT allowed us to generate frequency volumes to view and extract new information from seismic data. In the deepwater examples, SDT was applied for channel system delineation. This has improved our understanding of



The authors wish to thank Nigerian National Petroleum Corporation (NNPC) and Esso Exploration and Production Limited, Nigeria, for release of the materials and permission to publish this work. Many thanks to the Geoscience community of the Mobil Producing Nigeria Unlimited for technical reviews and suggestions.

reservoir architecture and connectivity, as well as Environment of Deposition (EOD). In the shallow water example, SDT was used to aid field-wide mapping of flat events associated with GOC and OWC. This provided improved confidence and accuracy in the mapping of seismic flat events, and ultimately, in the field-wide evaluation of future opportunities in the field.

In the following sections, we present a brief overview of theoretical concepts and explain the choice of SDT methods that were used in this study. Next, we discussed the field examples; highlighting technical impacts of the SDT integration. Finally, we summarize various learnings with recommendations for improved SDT integration into future opportunity generation studies in shallow JV and deepwater fields in Niger Delta and beyond.

## THEORETICAL CONCEPTS AND METHODS

An important underlying principle in SDT is the Fourier transform. In general, a seismic trace *g(t)* can be formulated as (Bracewell, 1986; Zhang *et al.,* 2009):

$$g(t) = \int a(t,f) e^{i\phi(t,f)}\, df \qquad (1)$$

where *a(t,f)* and $\phi$ *(t,f)* are amplitude and phase components, respectively, at time *f*. The Fourier transform *G(f)* of the seismic trace *g(t)* is the inner product of the signal with the basis function $e^{iwt}$ (Bracewell, 1986; Sinha *et al.,* 2005):

$$G(f) = \{g(t), e^{i\omega t}\} = \int_{-\infty}^{\infty} g(t) e^{-i\omega t}\, dt \qquad (2)$$

where $\omega = 2\pi f$ *t*. A seismic signal when transformed into frequency domain using the Fourier transform (Equation 2), gives the overall frequency behavior, in a stationary sense, over a large window representing entire spectrum of the signal (Bracewell, 1986). For spectral decomposition, the signal is 'windowed' (that is a short segment of the signal is taken) and Fourier transform is performed on the windowed data to obtain local frequency information. In other words, a window or kernel function (a filter) is introduced into Equation 2 such that (Sinha *et al.,* 2005):

$$G(f,\tau) = \{g(t), s(\tau)e^{i\omega t}\} = \int_{\infty}^{\infty} g(t)\bar{s}(t,\tau) e^{-i\omega t}\, dt \qquad (3)$$

where *G(f,*$\tau$*)* is a spectrally decomposed signal at analysis window $(t,\tau)$ (where $\tau$ is a window's parameter with $\bar{s}(t,\tau)$ being complex conjugate). Generally, different direct and analogous approaches have been proposed and applied to solve Equation 3 and its various adaptations. This has given rise to varieties of spectral decomposition methods for seismic data interpretation. Examples of these methods include: short time Fourier transform (STFT) (Partyka *et al.,* 1999); continuous wavelet transform CWT (Sinha *et al.,* 2005); the S-transform (Stockwell *et al.,* 1996; Odebeatu *et al.,* 2006); constrained least-squares spectral analysis (CLSSA) (Puryear *et al.,* 2012); Gabor transforms (Ying-Pin *et al.,* 2013); and matching pursuit spectral decomposition (Mallat and Zhang, 1993; Wang, 2007); among others. A comprehensive review of various spectral decomposition techniques is presented by Tary *et al.,* (2014).

According to Castagna and Sun (2006), SDT can be categorized as 'useful' or 'not useful' for the specific applications, and not as 'right' or 'wrong'. All the techniques have characteristics merit or demerit and different techniques are required or could be more suitable for different applications (Chakraborty and Okaya, 1995). Generally, successful applications of each of these methods for structural and stratigraphic interpretations have been documented (for examples: Partyka *et al.,* 1999; Hall and Trouillot, 2004; Odebeatu et al., 2006). For numerical implementation, Equation 3 (or any equivalent continuous function, depending on the SDT approach), is converted into discrete form (such as Discrete Fourier Transform) and algorithms are developed and packaged into user-friendly software. Presently, proprietary and commercial software are available such that, following initial seismic data conditioning and noise reductions, little data preparation or effort is required to get results to enhance geoscientists understanding of reservoir architecture. With present advances in technology, the practice is to test different techniques, and the method(s) for which target objectives are met is/are selected.

The frequency decomposition workflow that was adopted in this study was based on the deconvolution of Gabor wavelet with seismic trace (McArdle and Ackers, 2012) (for the deepwater studies), and CLSSA method (Puryear *et al.,* 2012) (for the fluid contact mapping). The methods were selected after initial evaluation of various SDT methods as implemented in the software that was available for this study. We decomposed the seismic volumes into a suit of frequency cubes and then view cross-sections and horizon-based slices extracted from different frequency cubes. The optimal frequency bands upon which the target geological features were best illuminated were selected. We used the RGB (Red, Green, and Blue) display scheme as applied by Liu and Marfurt (2007) to view the high, middle and low frequency slices in a single colour image. The RGB blending workflow assigned low frequency in the Red channel, mid frequency in the Green channel, and high frequency in the Blue channel. Generally, high frequency components are sensitive to the thin layers and low frequency components are better at revealing thick layers (McArdle and Ackers, 2012). Therefore, by combining different frequency components, we could better delineate channels with different thickness (Partyka *et al.,* 1999). Also, as part of the study, we generated RGB blended frequency volumes. This allowed shallower and deeper anomalies to be discovered, thereby generating additional opportunities for future studies.

## FIELD EXAMPLES

### Deepwater: Channel System Delineation

The SDT was applied to channel system delineation in two deepwater fields, offshore Niger Delta. The target reservoirs are JQ3 and BX4 reservoirs from separate geological settings.

Reservoir JQ3 consists of low impedance sands within a stratigraphically/structurally trapped mud rich turbidite system, in a mid-lower slope setting on the western flank of a shale-cored anticline structure. It consists of four weakly confined deepwater channel complexes trending NE-SW (Fig. 1). The reservoir is Upper Miocene in age and is composed of fine-grained amalgamated channel sands derived from the shelf margin. Estimated ultimate recovery for the reservoir is 130 MBO. Seismically, the reservoir is tuned as net reservoir thickness is expressed as single seismic loop events on seismic data. Figure 1a is an attribute extraction showing the reservoir deepwater channels and sample well locations. I1/P1 and I2/P2 injector/producer pairs were drilled in Channel B, whereas I3/P3 pair was drilled in Channel C. Ongoing studies seek for additional drill well opportunities in Channels A, B, C, and D. However, connectivity and sweep remain key uncertainties in development of JQ3 reservoir, making it critical to target injector/producer pairs in the same channels in the different regions.

Figure 1b shows RGB blended frequency data draped on a reference horizon representing the top of the reservoir. We obtained 14 frequency cubes in the usable frequency band, 5 - 60 Hz, at an interval of 5 Hz. The low, middle and high frequency components are at 15 Hz, 25 Hz and 35 Hz respectively, after careful inspection of different frequency volumes. The RGB blend reveals more detail about the channel systems, highlighting associated facies and resolving internal geometries. For examples, the occurrences and geometries of late stage channel systems, especially in Channels B and C, are highly visible. New insight provided by SDT has led, in part, to interpretation that performance of the various injector/producer pairs might have been impacted by the highlighted late stage channel systems. Also, noticeable is connection between Channels B and C (Figure 1b), which were initially and otherwise thought to be entirely separated based on attribute extractions (Fig. 1a). This information is currently being integrated into well placement decisions. In addition, a good correlation has been established between well data and spatial spectral expressions on the SDT-derived RGB surface (Figure 1b). Based on well data, areas of strong and equal response from the three decomposition frequencies which appear white, correspond to sandier areas, whereas dark color, with no resulting signal at any of the chosen frequencies of the blend (McArdle and Ackers, 2012), corresponds to low net-sand areas. This information corroborates results from amplitude extraction where brighter amplitudes correspond to thick net-sands (Fig. 1a). Generally, future

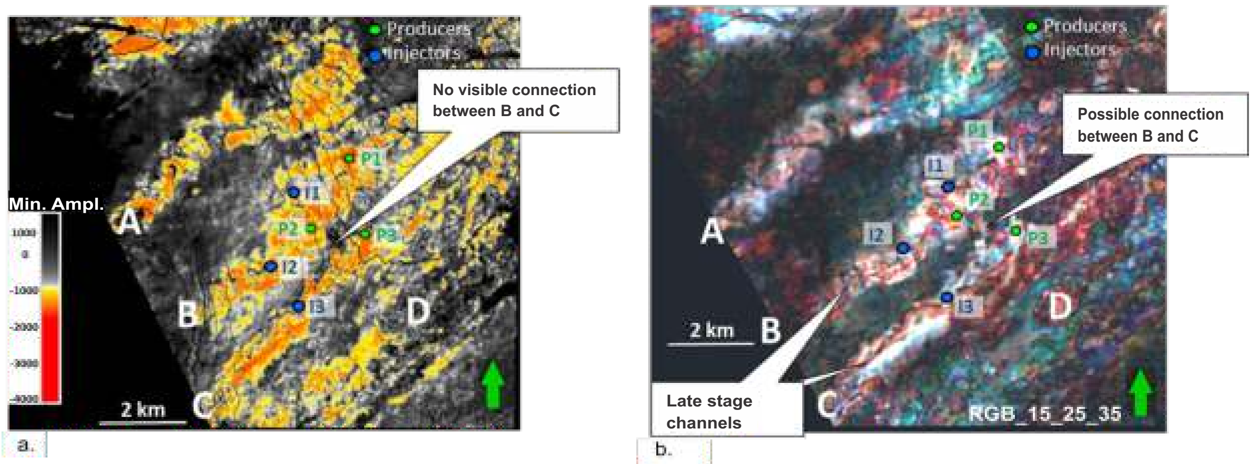


**Figure 1:** Reservoir JQ3 showing the producer/injector pairs; (a) amplitude extraction; (b) SDT-derived horizon-based color blend of 15 Hz, 25 Hz, and 35 Hz frequencies, as Red, Green and Blue colours, respectively.

drill wells are being designed to target relatively thick sands, where producer/injector pairs are well connected for sustainable pressure support.

The second case study was taken from another deepwater setting in the Niger Delta. Reservoir BX4 is an Upper Miocene sand located in a deepwater slope channel complex system. The reservoir consists of two separate fault blocks separated by a major fault. The downthrown block is penetrated by well E1X, which encountered oil in the Upper Miocene sand. Previous detailed study (Amidu *et al.,* 2015) used well and seismic data calibrations at E1X to de-risk fluid type in the unpenetrated fault compartment in the SW fault block. Results predicted oil in upper part of the unpenetrated SW fault block close to major fault. Also, previous wedge modeling has shown that reservoir thickness is relatively below the limit of seismic resolution (Amidu *et al.,* 2015).

extraction (Figure 1a) and SDT-derived surface (Fig. 1b). Overall, SDT enhanced better knowledge of internal architecture of the reservoir. The SDT information corroborates results from previous study (Amidu *et al.,* 2015), where a drill well location was proposed in upper side of the unpenetrated SW fault block close to major fault.

Beyond the horizon-based analysis, Figure 3 shows the blended 3D frequency volumes that were generated from above highlighted studies. These volumes provided opportunity for quick reconnaissance to identify anomalies away from the zones of interest. Generally, with such 3D volumes, entire field could be studied, where shallower and deeper anomalies could be mapped at resolution higher than could be possible with conventional time-domain seismic volumes. Details of such analysis, however, are beyond the scope of the

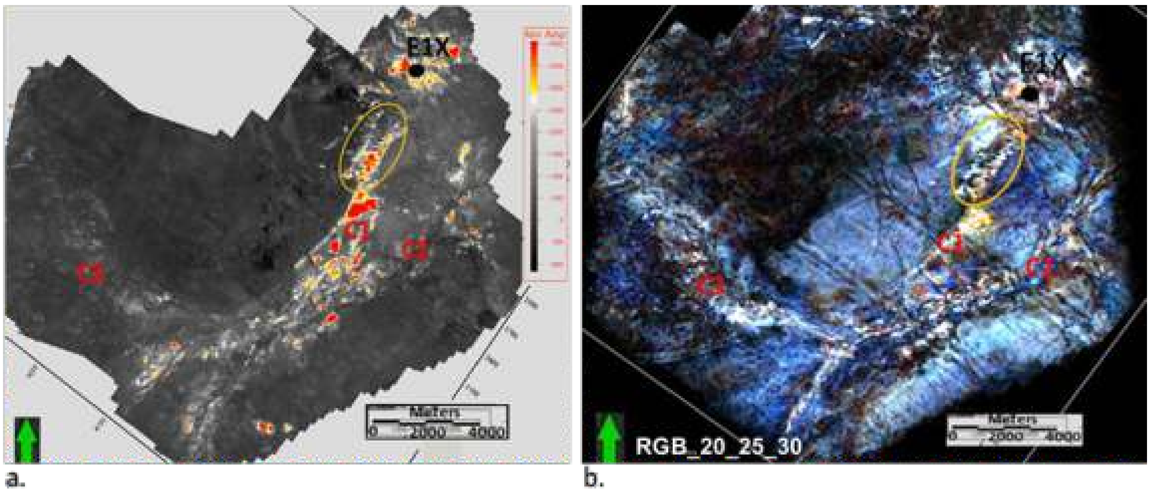


**Figure 2:** Reservoir BX4 showing deepwater channels and well E1X; (a) amplitude extraction; (b) SDT-derived horizon-based color blend of 20 Hz, 25 Hz, and 30 Hz frequencies.

Figure 2 shows an amplitude extraction and a horizon-based SDT-derived RGB blended frequency data from the reservoir. Improved level of details of channel patterns and locations of major faults are revealed by spectral decomposition. Two systems of channels (designated as C1 and C2) could be more clearly observed to run from NE to SW, where they merged to form bigger channel systems in the south. Also, SDT surface (Fig. 2b) shows detail geometry of branching channel C3, which was less visible in the attribute extraction (Fig. 2a). The proposed oil sand as inferred from previous study is within Channel C1 (yellow circle). The areal extent of the sand could be corroboratively inferred from both the amplitude

present study.

**Shallow Water: Fluid Contact Mapping**

We applied SDT to support presence of flat events, and to accurately map OWC and GOC on seismic volumes from BWY field in shallow water offshore Niger Delta. The field is one of the largest assets in the Niger Delta covering over 15000 acres, with over 200 wells, and a remaining reserve estimate of about 500 MBO. To effectively and accurately assess future opportunities in the field, field-wide mapping of fluid contact using seismic data was carried out.

We generated frequency volumes over a frequency range of 5 to 60 Hz at 5 Hz increment, and volumes for which the flat

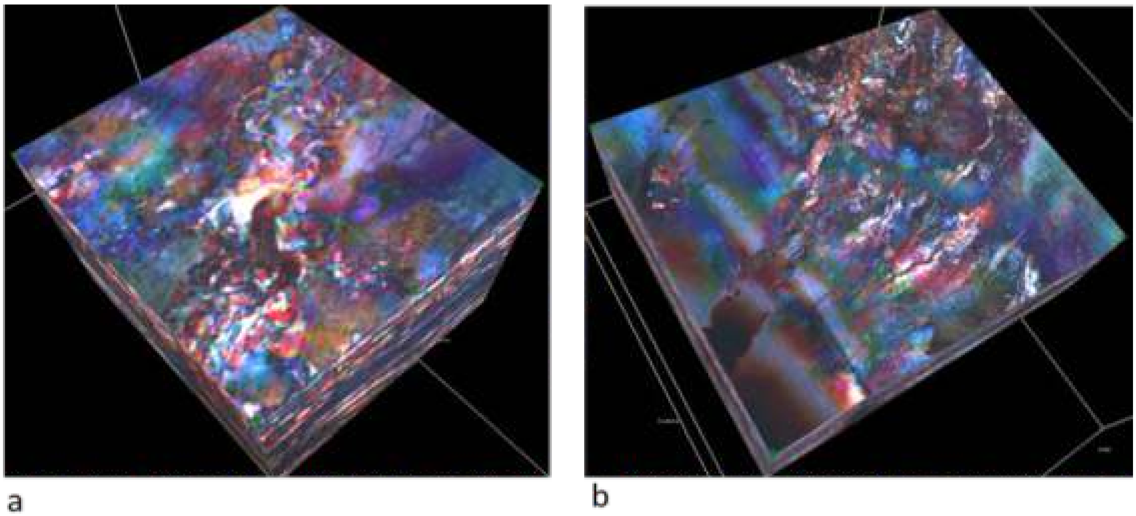


**Figure 3:** Examples of 3D SDT-derived RGB color blended volumes, which have been useful for field-wide quick reconnaissance to identify shallower and deeper anomalies.

events were most visible were selected. Figure 4a, shows examples of cross sections through the original seismic volume and the frequency data. The interpreted GOC and OWC are visible on all the displays, though careful analysis of the various sections reveals subtle difference in information in the seismic volumes. Generally, the frequency volumes were used interactively with the stacked time-domain volume for the fluid contact mapping. By integrating all the data, both the GOC and OWC could be better mapped with confidence throughout the field.

Figure 4b shows the originally mapped GOC and OWC, whereas Figure 4c shows SDT assisted maps of the fluid contacts for the field. The advantage of SDT integration into the work process is clearly visible. The SDT allowed the contact to be densely mapped, as the SDT integration allowed the flat events to be mapped with improved confidence; thereby increasing accuracy of results. The field-wide estimation of remaining oil column thickness was eventually carried out using the GOC and OWC maps. Relatively un-swept areas were characterized by higher oil column thickness, whereas low oil thickness correlated to areas with higher production impact. Results were consistent with available static and dynamic models for the field. Overall, this information has aided evaluation of remaining oil reserves, drill well planning, production optimization, and general future opportunities in BWY field.

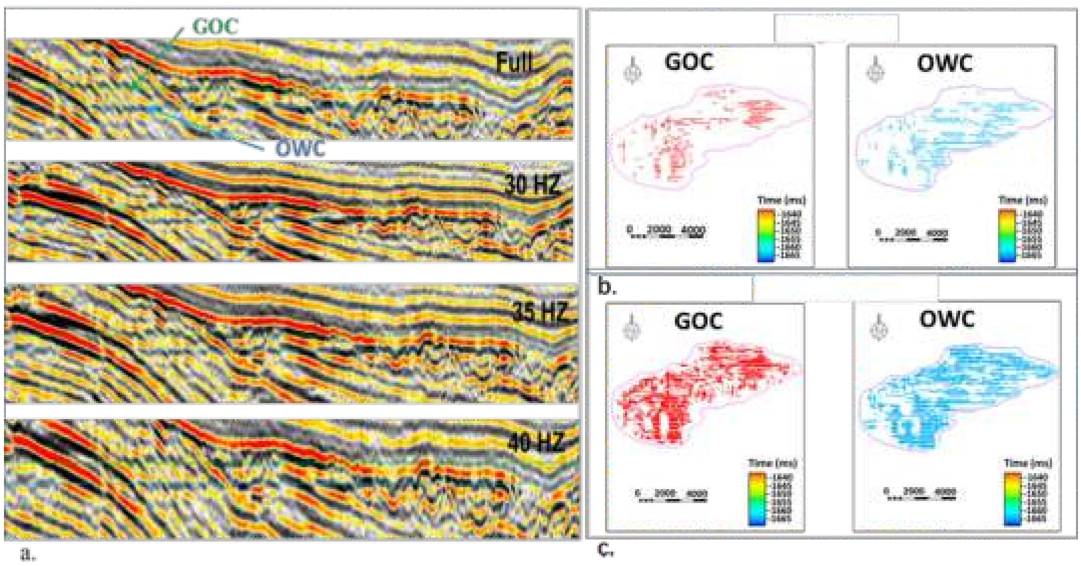


**Figure 4:** SDT-derived technical products for BWY field; (a) Seismic cross sections through original seismic data and frequency volumes; (b) Basemap display of mapped GOC and OWC flat events as mapped from time-domain volume; (c) Basemap display of mapped GOC and OWC flat events assisted with SDT-derived frequency volumes.

## SUMMARY AND CONCLUSION

Spectral decomposition analysis is an important imaging tool for reservoir characterization. Three field examples presented illustrate how high-resolution picture of a reservoir can be built with greater confidence to obtain better understanding of risks and uncertainties. In the deepwater examples, SDT enhanced stratigraphic details not obvious in traditional amplitude extractions. Results have improved understanding of the reservoirs architecture and thereby reducing reservoir connectivity uncertainties. For the shallow water environment case study, integration of SDT helped to improve confidence in the field-wide mapping of flat events associated with fluid contacts, and thereby enhancing accurate evaluation of future opportunities in the BWY field.

In addition, ability to generate RGB-blended 3D frequency data has helped to identify anomalies that could be the focus of future studies. With current advances in technology and availability of proprietary and commercial software, following initial data conditioning, little effort is required to get results to enhance better understanding of reservoir architecture. Nevertheless, a good knowledge of SDT fundamentals coupled with knowledge of reservoir of interest will help to guide choice of methods and ensure accuracy of SDT-derived data interpretation. Generally, improved SDT integration into shallow and deepwater studies is recommended to extract subtle information from seismic data. Presently, the technology is currently being used to support other ongoing projects in our shallow JV and Deepwater fields; adding confidence to stratigraphic and structural interpretation.

## REFERENCES CITED

Amidu, S. A., Ochogbu, P. I., Medema, G. F., Obere, F. O., and Drexler, C. W., 2015, De-risking fluid type in unpenetrated fault compartment using seismic calibration, Erha Field, offshore Nigeria, Nigerian Association of Petroleum Explorationists, 33rd Annual International Conference and Exhibition, Extended Abstract, Lagos, Nigeria.

Bracewell, R, 1986, The Fourier transform and its applications, McGraw-Hill Publishing Company, 2nd Edition

Burnett, M., Castagna, J., Méndez-Hernández, E., Rodríguez, G., García, L., Vázquez, J., Avilés, M., and Villaseñor, R., 2003, Application of spectral decomposition to gas basins in Mexico, The Leading Edge, 22 (11), P1130–1134.

Castagna, J., and Sun, S., 2006, Comparison of spectral decomposition methods, First Break, 24, P75-79.

Chakraborty, A. and Okaya, D., 1995, Frequency-time decomposition of seismic data using wavelet-based methods, Geophysics, 60, P1906–1916.

Hall M. and Trouillot E., 2004, Predicting stratigraphy with spectral decomposition, CSEG, National Convention Abstracts, Volume, June 2004.

Liu, J. L., and Marfurt, K. J., 2007, Instantaneous spectral attributes to detect channels: Geophysics, 72(2), P23–P31, doi:10.1190/1.2428268.

Mallat, S., and Zhang, Z., 1993, Matching pursuit with time frequency dictionaries, IEEE Trans. signal prec., 41, P3397 - 3415.

Marfurt, K. J., and Kirlin, R. L., 2001, Narrow-band spectral analysis and thin-bed tuning: Geophysics, 66, P1274 - 1283.

McArdle, N., and Ackers, M., 2012, Understanding seismic thin-bed responses using frequency decomposition and RGB blending.First Break, 30, P57-65.

Odebeatu, E., Zhang, J., Chapman, M., Liu, E., and Li, X., 2006, Application of spectral decomposition to detection of dispersion anomalies associated with gas saturation, The Leading Edge, 25(2), P206–210.

Partyka, G., Gridley, J., and Lopez, J., 1999, Interpretational applications of spectral decomposition in Reservoir characterization, The Leading Edge, 18(3), P353–360.

Puryear, C. I., Portniaguine, O. N., Cobos, C. M., Castagna, J. P., 2012, Constrained least-squares spectral analysis: Application to seismic data, Geophysics, 77(5), P143167.

Sinha, S., Routh, P., Anno, P., and Castagna, J., 2005, Spectral decomposition of seismic data with continuous-wavelet transform, Geophysics, 70(6), P19-25.

Tary, J. B., Herrera, R. H., Han, J., and van der Baan, M., 2014, Spectral estimation - What is new? What is next?, Reviews of Geophysics (American Geophysical Union), 52(4), P723-749, doi: 10.1002/2014RG000461.

Wei, X. D., 2010, Interpretational applications of spectral decomposition in identifying minor faults, EAGE 72nd Conference and Exhibition, Extended Abstracts, D023.

Ying-Pin, C., Zhen-Ming, P., Zhen-Hua, H., Lin, T., and Dong-Jun, Z., 2013, The optimal fractional Gabor transform based on the adaptive window function and its application, Applied Geophysics, 10(3), P305-313

Yoon, W., and Farfour, M., 2012, Spectral decomposition aids AVO analysis in reservoir characterization: A case study of Blackfoot field, Alberta, Canada, Computers and Geosciences, 46, P60-65.

Zhang, K., Marfurt, K. J., Slatt, R. M., and Guo, Y., 2009, Spectral decomposition illumination of reservoir facies,Society of Exploration Geophysicists, International Exposition and Annual Meeting, Houston, Texas, Extended Abstracts, P3515-3519

# Foraminiferal Analysis and Palaeoenvironmental Reconstruction of Sediments in Amofu, Southern Benue Trough, Nigeria

**Courage Ewezugachi Ugwuanyi, Ikenna Chris Okwara and Charles Chibueze Ugbor**
Department of Geology, University of Nigeria, Nsukka

## ABSTRACT

The nature and distribution of potential resource-bearing rocks are key in geological exploration. Palaeogeographic reconstruction of sedimentary basins provide important information on the prevailing environmental conditions during their deposition and hence serves as potential resource indicator. This study focuses on areas around Amofu, present-day Enugu state, Southern Benue Trough, Nigeria. Detailed Geologic mapping involving lithologic description was undertaken in order to decipher the underlying rock types and stratigraphy. Also micropalaeontological analysis was carried out on representative samples from the area to ascertain the foraminiferal biostratigraphy, establish the age of the rocks, and interpret the palaeodepositional environment of the area. The area is underlain by shale, heteroliths of shale-siltstone and shale-sandstone, and sandstone units. Twelve planktonic foraminiferal species were recovered (Guembelitria cenomana, Guembelitria cretacea, Heterohelix moremani, Heterohelix globulosa, Heterohelix reussi, Hedbergella delrioensis,, Hedbergella planispira, Hedbergella simplex, Whiteinella archeocretacea, Whiteinella baltica,. Whiteinella aprica, and Whiteinella inornate). Only planktonic foraminiferal species were present, indicating essentially open marine environment. The preponderance of calcareous tested species also indicates shallow marine conditions. Other microfossils recovered include gastropod Turritella and Ostracod. Based on diagnostic short-ranged foraminifers of the Whiteinella and Guembelitiria species recovered, an age of Mid Aptian to Latest Turonian is assigned to the rocks in the study area. Integrated field, micro-, and trace fossil assemblage studies overall suggest a lower shoreface palaeodepositional environment, with a low thermal gradient, reduced water mass stratification, and a well-developed oxygen minimum zone.

**Keywords:** Foraminifera**,** Palaeodepositional Environment, Stratigraphy, Microfossil, Lithostratigraphy, Palaeogeography

## INTRODUCTION

Palaeogeographic reconstruction of sediments in sedimentary basins provide important information on the prevailing environmental conditions during their deposition and hence serves as potential resource indicator. It often requires determination of spatial and temporal distribution as well as relationships of strata that generally represent diverse environments of deposition. Integrated lithostratigraphic and biostratigraphic studies, as well as sequence stratigraphic analysis are very important tools that aid a much reliable paleogeographic reconstruction (Tew and Mancini, 1995). The intensive studies of foraminifera in sediments of Southern Benue Trough during the last two decades have proved them to be very useful for regional correlation to ascertain palaeoenvironments of deposition and age determination over the Cretaceous period.

Detailed geologic mapping and lithologic description were carried out at Amofu and the environs, in the present day Enugu state. It lies within the Abakaliki basin, southern Nigeria (Fig. 1). It is bounded by latitudes 6º 05´N to 6º 10´N of the equator, and longitudes 7º 40´E to 7º 45´E of the Greenwich Meridian, covering an area of 85.56 km2 (Fig. 2). Foraminiferal assemblages from the clastic sediments in the area were recovered and analyzed. The present geological study was undertaken to assess the lithofacies and biofacies within the area to ascertain the foraminiferal biostratigraphy, establish the age of the rocks, and reconstruct the palaeodepositonal environment in which the sediments in the area were deposited.

### Geological Setting

The Southern Benue Trough, in which the Abakaliki basin is located, is an elongate NE-SW trending intracratonic depression, with length of over 1,000 km and width of about 250 km (Nwajide, 2013) flanked on either side by Precambrian rocks. The elongated appearance of the



We wish to show appreciation to the Department of Geology, UNN for allowing us use its Palaeontology Laboratory for our work. Our sincere gratitude to Dr. Dim C.I.P., whose work around the study area, gave much insights and helped in the development of this study.

NAPE Bulletin, V.29 No 2 (November 2020) P. 26-42

trough tends to suggest some sort of structural control for its formation, hence has led to a number of propositions, ideas or models for its origin and evolution. These and more recent models based on modern concepts of plate tectonics are well documented in the works of Wright (1968), Grant (1971), Burke *et al.,* (1971, 1972), Olade (1975), Ofoegbu (1984) and Benkhelil (1986). Three major tectonic events have been identified in Southern Benue Trough. They include the Albian phase, the second Santonian thermal phase and the third Eocene structural inversion event. These are well recorded in Short and Stauble (1967); Murat, (1972); Obi *et al.,* (2001). Of the three tectonic events, the Santonian compressive movement, terminated sediment deposition in the Abakaliki basin. It resulted in folding, uplift, faulting, magmatism, and creation of the Abakaliki Anticlinorium, which laterally translated the depocenter westward and eastward forming

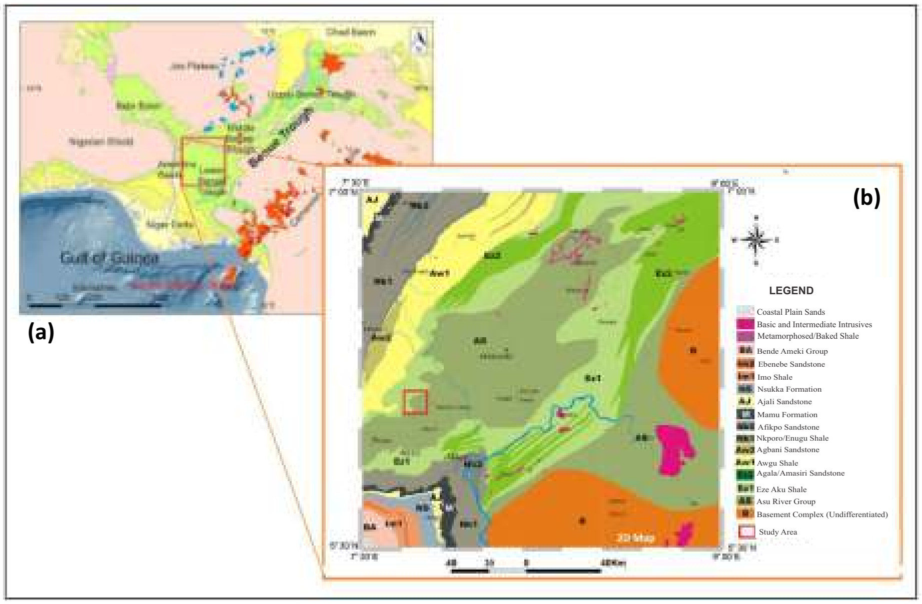


**Figure 1: (a)** Map of Nigeria showing the location of the Southern Benue Trough (adapted from Abdullahi *et al*., 2019**)**
**(b)** Geologic map of the Southern Benue Trough showing the location of the study area (adapted from Dim *et al.*, 2016).

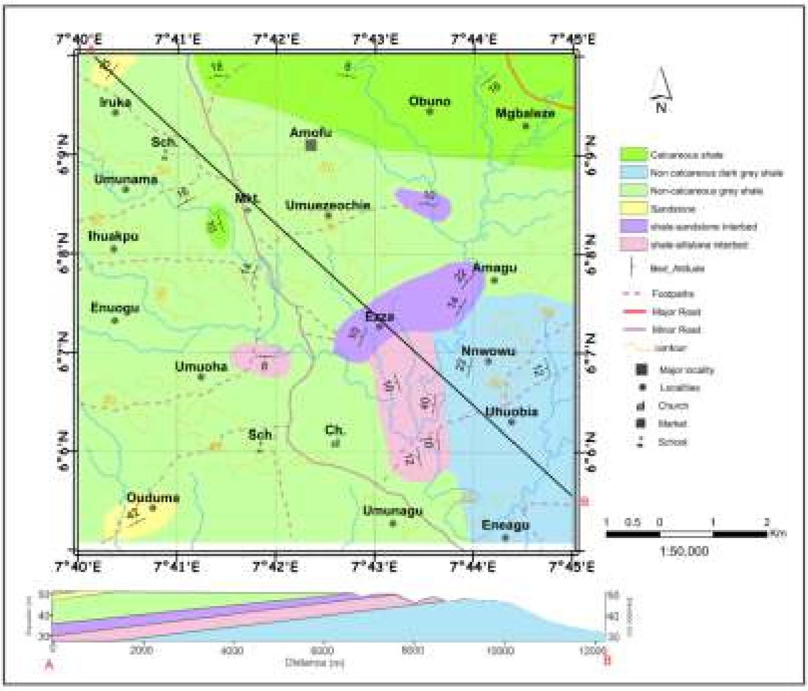


**Figure 2:** Geographic (accessibility, relief and drainage), geologic map (outcropping lithogies and litostratigraphic units) and Geologic cross-section (A–B), across the study area.

the younger Anambra and Afikpo basins respectively (Nwachukwu, 1972; Benkhelil, 1982).

Thus, the stratigraphic succession of the Abakaliki Basin is pre-Santonian in age and has been established as the Asu River Group, Eze-Aku Group and Awgu Formation (Table 1). The stratigraphic successions and sedimentologic history of the basin are well documented in Hoque (1976) and Ojoh (1992). The Albian Asu River Group comprises the oldest marine deposits in the Southern Benue Trough. It consists dominantly of very thick, dark grey shales, which are typically calcareous, with subordinate fine-grained, micaceous sandstones, micaceous siltstones and limestones (Cratchley and Jones, 1965). This Eze-Aku Group comprises thick flaggy calcareous shales, bluish non-calcareous shales, sandy or shelly limestones and calcareous fine to medium-grained sandstones (Reyment, 1965, Umeji, 2000). The Awgu Formation overlies the Eze-Aku Group and consists of greyblue shales, with subordinate limestones and calcareous sandstones whereas the Agbani Sandstone is made up of a medium- to coarse-grained bioturbated sandstones. The Awgu Shale contains Turonian foraminiferas at its base and Coniacian ammonites at its top (Benkhelil, 1986).

## MATERIALS AND METHOD OF INVESTIGATION

The study approach involved both field data outcrop mapping, and analyses of data. Study tools include compass, topographic maps obtained from Nigerian Geological Survey Agency (NGSA), GPS, geological hammer, sample bags, dilute acid and field notebook. The software employed include GIS software, (ArcGIS), sedimentological logging tool, (SedLogTM 3.1), and Excel.

Twenty-Six outcrop locations were studied and sampled systematically essentially along river channels for the sedimentological, tectonic and biostratigraphic characteristics. The rock records were further subjected to various analyses for presentation. The lithologic succession was represented using SedLog TM 3.1. This was followed by detailed facies analysis to aid paleo-environmental interpretation. Representative shale samples collected from outcrop sections from 6 locations were taken to the laboratory for micropalaeontological studies in the Organic Chemistry Laboratory, Department of Geology, University of Nigeria. The preparation of the samples in the laboratory for micropalaeontological analysis strictly followed standard procedures (Armstrong and Braisier, 2005).

Fifty grams of each sample was weighed using a weighing balance and then dissolved in a beaker containing kerosene. This was allowed to stand for 48 hours, after which the kerosene was decanted and water was added to the beaker such that the sample was completely submerged and allowed for 24 hours. Each dissolved sample was washed in a 63 micron sieve mesh with the aid of jet stream of water and detergent, until all the mud was completely removed. The shale residues containing

**Table 1:** Stratigraphic succession in the Abakaliki Basin (Sourced and Redrawn from Dim *et al.,* 2016).

Generalized Stratigraphic Chart of the Abakaliki Basin Souther Benue Trough

| BASIN | | FORMATION | AGE | | ENVIRONMENT | DEPTH | SANDSTONE PETROLOGY | TECTONO. SEDIMENTOLOGIC STAGE |
|---|---|---|---|---|---|---|---|---|
| CRETACEOUS | ABAKALIKI | AWGU GROUP (Awgu Formation/ Agbani sandstone/ Nkalagu Formation) | CONIACIAN | | MARINE | | FELDSPATHIC SANDSTONE | DEFORMATION STAGE |
| | | | TURONIAN | UPPER | MARINE | 1000m | | TROUGH STAGE |
| | | | | MIDDLE | SHELF | 1150m | | |
| | | EZE-AKU GROUP (Eze-Aku shale/ Agaila/Makurdi/ Amaseri sandstone/Ibir sandstone) | | LOWER | MARINE | 1350m | | |
| | | | CENOMANIAN | UPPER | MARINE | 1500m | | |
| | | | | MIDDLE | MIXED | | | |
| | | | | LOWER | SUBCONTINENTAL | | | |
| | | ASU-RIVER GROUP (Abakaliki shale/ Minor intrusions) | UPPER ALBIAN | LATE | NEARSHORE | 1880m | | |
| | | | | MIDDLE | INTERNAL AND EXTERNAL SHELF | 1980m | | |
| | | | | EARLY | | | | |
| | | | MIDDLE ALBIAN | | MARINE BASIN | 2130m | | |
| | | NOT OUTCROPPING ? | PE-MIDDLE ALBIAN (Aptian, Ncocomian) | | DELTAIC | 3630m | | RIFTING STAGE |
| | | | | | NON MARINE | | | |
| | | MAJOR DISCORDANCE | | | METAMORPHIC | 5000m | | |
| | PRECAMBRIAN BASEMENT | | | | | | | |
| After Ojoh, 1992: Petters, 1991 and Murat, 1970. | | | | | | | After Hoque and Nwajide, 1985 | |

fossils were allowed to dry for 24 hours. The dried samples were poured into fossil plate for fossil identification under the paleontological binocular microscope. Fossils were picked using picking brush based on its diagnostic forms and placed in a fossil box for more detailed description. Precautions taken to avoid contamination of samples include rewashing of the sieve mesh after sieving a particular sample and cleaning up the fossil plate and picking brush after each use. A comprehensive foraminiferal album was used as guide in the identification, naming and description of the fossils. The information obtained was plotted on a foraminifera distribution chart. The age determination of the sediments in the area was based on the use of last appearance datum and first appearance datum of age diagnostic foraminiferal species. Identification of species assemblage that represent a particular depositional environment was also carried out during the biofacies analysis.

## RESULTS AND DISCUSSION

### Lithofacies Analysis

The results show 4 distinguishable lithofacies based on lithology, colour, grain size, texture and sedimentary structures. They are: (1) shale facies (F 1); (2) heterolithic shale-siltstone facies (FA 2); (3) shale-sandstone facies (FA 3); and (4) sandstone facies (FA 4) (Fig. 3).

### Shale Facies (F 1)

**Description:** The shale facies (F 1) is the most common facies in the area and has two subordinate lithofacies. These are the calcareous shale (F 1a) and non-calcareous shale (F 1b) sub-lithofacies. The calcareous shale (F 1a) sub-lithofacies are generally dark grey, fissile, moderately to highly indurated and calcareous (Fig. 4a). At some locations they are micaceous, appear as grey to yellow or yellowish brown and intensely fractured, resulting in a closely spaced fracture network (joint set). The fractures trend generally in the NNE-SSW direction. The beds are generally tilted with dip amounts ranging from 80 to 180 and varying dip directions towards NNE, SSW and NNW. A well-developed exposure of the calcareous shale sub-lithofacies is along the Asu-River in Umuezeochie, where it extended laterally for about 35 m and consists of alternations of "thin" fissile shale beds with relatively "thick" moderately-indurated shale beds. The thin beds are 8-10 cm thick, while the moderately indurated shale beds are 0.7-1 m thick.

The non-calcareous shale (F 1b) sub-lithofacies have been grouped into two based on variation in colour, namely: *dark grey non-calcareous* shales (F 1b-dg) and *grey non-calcareous* shales (F 1b-g). The colour may also be suggestive of organic matter enrichment and environmental conditions during deposition. A good representative of the *dark grey non-calcareous shale (F 1b*-dg*)* is at Nwowu. Here, it consists of alternations of very thin (6-8 cm) moderately indurated micaceous dark grey mudstones with about 20 cm thick fissile, dark grey shale, having an overall thickness of approximately 2 m (Fig. 4b). At some other locations, the dark grey non-calcareous shales are well exposed, fractured but lack bedding planes. The *grey non–calcareous shales (F 1b-g)*

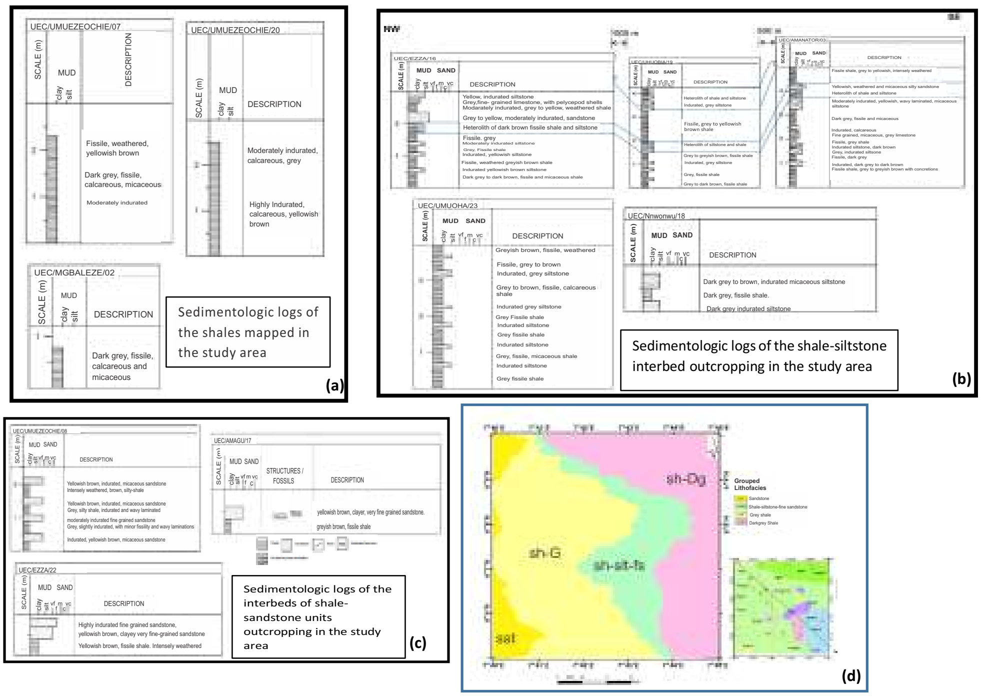


5 **Figure 3:** (a)-(c) Sedimentological Logs of various Outcrop Sections Mapped in the study area. (d) Lithofacies Map showing the various Lithofacies (inset: geologic map (outcropping lithogies and litostratigraphic units)).

in most places are weathered, appear grey to yellowish brown, fissile and fractured. The representative section of this sub-lithofacies occur at Ihuakpu, along Evu River.

**Interpretation:** The deposition of shales indicates settling from suspension in a very low energy setting. The dark grey shales (F 1a) and (F 1b-dg) indicate presence of organic matter under reducing conditions. The occurrence of calcareous shales (F 1a) suggests a shallow marine environment, rich in marine life that have calcareous shells and skeletons. These shells and skeletons constitute calcareous materials from which calcium carbonate is made available during burial and dissolution by groundwater moving through the sediment. The alternation of shale with mudstone at Nwonwu suggests an alternation of periods of quiescence in water, which allowed gradual settling of the suspended clay-size particles in layers, thus forming the shales and the rapid influx and deposition of silt-sized particles alongside clay-size particles giving rise to the mudstones.


**Figure 4**: **(a)** Dark grey, fissile calcareous shale
**(b)** Non-calcareous shale at Nnwowu showing centimeter scale alternations of moderately indurated mudstones with fissile shale.

**Heterolithic Shale-Siltstone Facies (F 2)**

**Description:** This facies consists of repeated interbedding of dark grey to greyish brown shales with moderately to highly indurated grey to yellowish brown siltstones. The shale bed thickness varies at different locations with an average thickness of 0.5 m, while the siltstone beds have an average thickness of 0.1 m. The beds generally tilt at angles ranging between 80 and 120, with beds oriented in the NNW-SSE direction, dipping towards WSW. The exposed sections at Amanator, Ezza and Uhuobia have occurrences of shale and siltstone heterolithic units within a distinct shale-siltstone interbed (Fig. 5). However, at Amanator, the heterolithic unit overlies a 0.7 m thick wavy laminated siltstone. In addition, the exposures at Amanator and Ezza comprise subordinate (10-30 cm thick) greyish fine-grained, fossiliferous limestone (Fig. 6). Body fossils observed are sparse pelecypod shells.

**Interpretation:** The shale-siltstone interbed suggests an overall low velocity regime with minute changes in energy due to occasional sea-level fluctuations. Heterolithic units could be the result of fluctuations in sediment supply and tidal velocity. The wavy-laminated siltstone just below the heterolithic unit at Amanator, suggests wave influenced sediment just below the fair-weather wave base, which are typical of lower shoreface. The associated limestone beds with the succession of siltstones with shales in the area may be due to periods of low supply of terrigenous clastic detritus and availability of calcium carbonate at that time. The body fossil (pelecypod) present is indicative of marine environment and broken shell fragments may be due to wave action.

**Shale-Sandstone Facies (F 3)**

**Description:** The shale-sandstone facies (F 3) comprises interbeds of shale and sandstone. At Ezza, intensely weathered yellowish-brown fissile shale (0.4 m thick) is overlain by 0.3 m thick moderately indurated yellowish brown, clayey, very fine-grained sandstone, which is also overlain by 0.2 m thick highly indurated yellowish brown fine-grained sandstone, with intensely fractured bed top forming a dense fracture network, oriented essentially ENE-WSW and ESE-WNW directions. The shale-sandstone facies (F 3) also occurs as 2.2 m thick interbeds of grey to yellowish brown, moderately indurated, wavy laminated silty-shales with indurated fine-grained micaceous sandstones at Umuezeochie. The silty-shales are about 40 cm thick, while the sandstones are 20 cm thick (Fig. 6b). Notable among the exposures at Amagu, is a very low outcrop section comprising 0.4 m thick fine-grained, parallel laminated, fossiliferous sandstone overlying 0.3 m thick greyish brown, fissile shale (Fig. 6e). The trace fossils include intense bioturbation of bird-foot like trace of Chondrites at the top of the fine-grained


**Figure 5:** Exposed sections at **(a)** Amanator, **(c)** Ezza and **(d)** Uhuobia showing shale and siltstone heterolithic units, shale-siltstone interbed and limestone. NB: **(b)** zoomed in view of part of **(a).**

unit, and sub-horizontal to horizontal Planolites burrows of moderate to severe bioturbation intensity (Fig. 6c-d). Additionally, a pronounced exposure was also mapped at same location, comprising a 30 m laterally extensive (30 cm thick) highly indurated, yellowish-brown, fine-grained micaceous sandstone overlain by a shaly overburden of about 1 m thick. The sandstone has subtle internal parallel laminations and intensively fractured, with trends mainly in the ESE-WNW direction. The beds of the shale-sandstone facies (FA 3) generally dip WNW direction at angle ranging from 100 to 220 with strike in the NNE-SSW direction.

**Interpretation:** The wavy laminations on the silty-shales may have formed from movement of sediment as bedload by traction (or wave) currents at the onset of high velocity. The shale-sandstone succession at Umuezeochie suggests oscillations between low and high energy. The *Cruziana* ichnofacies are represented in nearshore marine and coastal environments (Pemberton *et al.,* 1992)**.** This ichnofacies association *(Chondrites and Planolites*) suggests a shelf area (sublittoral) environment where current action is less intense (Roy, 1978). The increasing grain size (coarsening upward) of the section at Ezza indicates increase in energy.

**Sandstone Facies (FA 4)**

**Description:** This facies consists of fine-grained, yellowish brown sandstones. They are intensely weathered and slightly indurated. Thickness vary from 1.5 m (with about 2 m thick overburden) at Ouduma to about 1.3 m at Iruka. The beds at Iruka are gently tilted at angles of 100, while those at Ouduma are steeply dipping at angles of 420 with strike in the ENE-WSW direction and dipping NNW.

**Interpretation:** The fine-grained sandstones indicate moderate energy environment. Sediment influx may have been as a result of wave action. The lack of sedimentary structures may be due to intense weathering of this unit or probably due to rapid deposition with less time to develop structures (Nichols, 2009).

**Biofacies Analysis**

The observed trace and body fossils contained in the rocks of the study area were analyzed, systematically grouped and described.

The trace fossils which occurred on fine-grained sandstone at Amagu are grouped ethologically as fodinichnia (sediment processor). Fodinichnia (deposit-feeding burrows) include the combined activities of


**Figure 6:** (a) Outcrop section at Umuezeochie showing alternations of fine-grained sandstone with wavy laminated silty shales. **(b)** zoomed in view of part of **(a).** **(c)** fossil trace: *Planolites* **(d)** fossil trace: *Chondrites* **(e)** Exposure at Amagu showing fossiliferous fine-grained sandstone.

feeding and dwelling in sediments and involves the systematic mining of sediments for food. The maintenance of open burrows by these deposit-feeding organisms that produce traces of fodinichnia is inferred as enabling them to exploit the rich organic matter content of the sediment while circulating dysoxic water through the burrow for respiration (Martin, 2004). The trace fossils observed belong to the ichnogenera, Chondrites and Planolites, which belong to the Cruziana ichnofacies. Intense bioturbation is common within the Cruziana ichnofacies, and this may reflect abundance and accessibility of food (Ekwenye *et al.,* 2016).

6 selected shale samples from six different localities were analyzed for body fossils (see Fig. 7 for sampled locations and points where samples were taken). Of the 6 samples, 2 samples were barren one 1 sample yielded an ostracod species (*Clithrocytheridea senegali*) and gastropod *Turritella* and only 3 samples yielded foraminiferal species indicating poor recovery. In spite of this, some samples were relatively rich in some forms, but quite depleted or near absent in others. In addition, the relative sizes of the foraminiferal species vary from one sample to another. There were also variations in abundance. A total of twelve planktonic foraminiferal species belonging to 4 genera were recovered. The planktonic genera include *Heterohelix, Whiteinella, Hedbergella,* and *Guembelitria***.** A brief description of the planktonic genera is presented in Table 2. The foraminiferal species recovered include *Guembelitria cenomana, Guembelitria cretacea, Heterohelix moremani, Heterohelix globulosa, Heterohelix reussi, Hedbergella delrioensis, Hedbergella planispira, Hedbergella simplex*, *Whiteinella archeocretacea, Whiteinella baltica, Whiteinella aprica,* and *Whiteinella inornata*. The distribution and diversity of the foraminiferal species within the fossiliferous analyzed samples are shown in Table 3.

**Systematic Ichnology of Trace Fossils**
**Ichnogenus:** *Chondrites*
**Type Ichnospecies**: *Chondrites isp* (Fig. 6d)
**Description:** This is a root-like structure with dendritic branching shafts and tunnels of uniform diameter ranging from 0.1 to 0.4 cm and the branching angle is relatively constant between 300 and 400. The burrows are generally clay filled.
**Ichnogenus:** *Planolites* Nicholson, 1873
**Type Ichnospecies**: *Planolites montanus* Richter, 1937 (Fig. 6c)

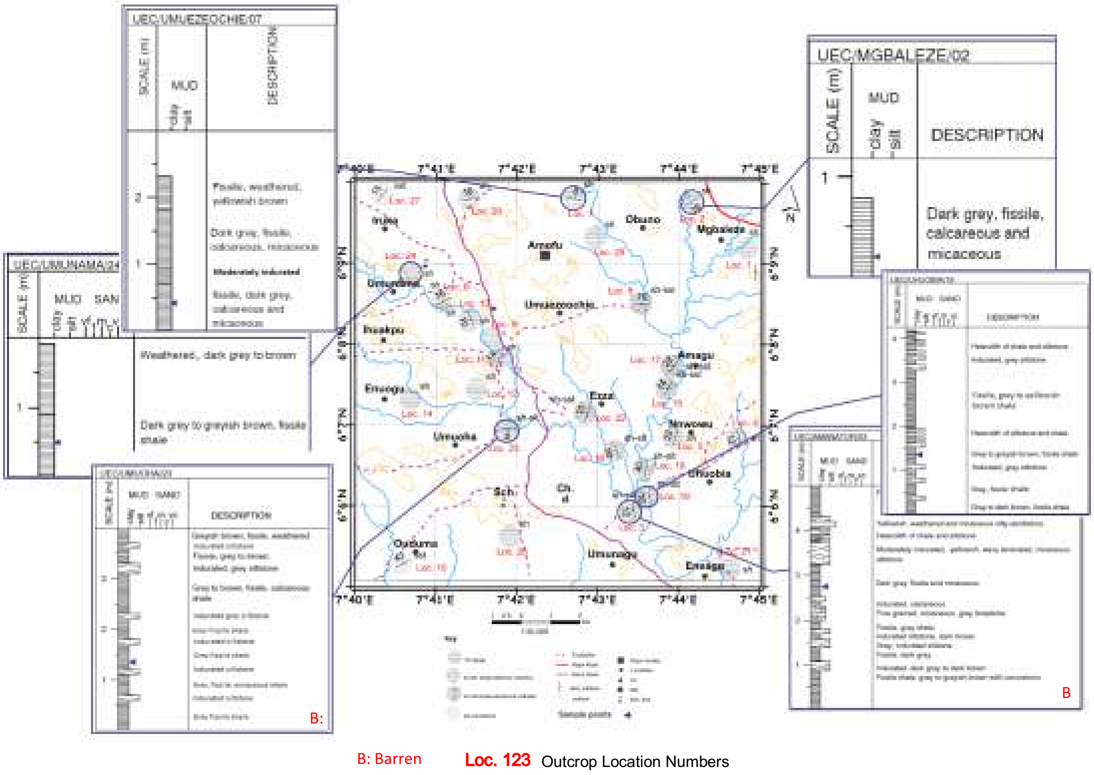


**Figure 7:** Map showing outcrop locations, lithologs of the outcrops and points from where samples were collected for micropalaeontology analysis.

**Description:** This consists of unlined, smooth walled, curved to straight cylindrical, unbranched burrows. The burrow fill is structureless, dark coloured and different from the host rock. Diameter of 3-5 mm and maximum length of 10-20 cm.

**Systematic Description of Foraminiferal Species**

**1. Genus: *Guembelitria*** Cushman, 1933**.**

**A. Type species**: ***Guembelitria cenomana*** Keller, 1989 (Fig. 8)

**Description**: Test is free, small, triserial throughout. Chambers are globular and inflated. Sutures are distinct and depressed. Aperture is a low interiomarginal arch at base of last chamber. Maximum height is 120 microns, maximum width 40 microns.
**Stratigraphic range:** Middle Albian to Earliest Turonian (Hart *et al.,* 1981)

**B. Type species: *Guembelitria cretacea*** Cushman, 1933 (Fig. 8)

**Description:** Test is triserial, elongate and its surface decorated with pore mounds. The species differs from *G. cenomana* in having a higher apertural arch.
**Stratigraphic range:** Middle Albian to Earliest Turonian (Hart *et al.,* 1981)

**2. Genus: *Heterohelix*** Ehrenberg, 1843**.**

**A. Type species: *Heterohelix moremani*** Cushman, 1933 (Fig. 8)
**Description:** Test is free, small, slender, consisting of 6-9 pairs of chambers, which are uninflated and very gradually increasing in size. Test is also biserial and gently tapering.

Aperture is a low interiomarginal arch formed at base of last chamber, bordered by a narrow imperforate lip. Maximum length is 120 microns, maximum width 50 microns.
**Stratigraphic range:** Middle Albian to Late Cenomanian (Hart *et al*, 1981).

**B. Type species**: ***Heterohelix globulosa*** Ehrenberg, 1978 (Fig. 8)

**Description:** Test is free, small and biserial. Chambers globular, increasing rapidly in size as added, and test tapers towards base. Sutures distinct and depressed. Wall smooth to finely striate. Aperture is a low arch on the inner margin of the final chamber. Maximum length is 340 microns, width 200 microns.
**Stratigraphic range:** Cenomanian

**C. Type species: *Heterohelix reussi*** Cushman, 1933 (Fig. 9)

**Table 2:** Brief description of the foraminifera genera recovered from the analysed sample.

| Foraminifera Genera | Description |
|---|---|
| ***Heterohelix*** | Test either with a minute initial planispiral coil followed by a biserial stage, or biserial throughout |
| ***Whiteinella*** | It differs from *Hedber gella* in the presence of portici; from *Archaeoglobigerina* in the absence of tegilla and absence of the wide imperforate peripheral band; from *Praeglobotruncana* in the absence of imbricated pustules along the peripheral margin. *Whiteinella* is a homeomorph of *Globotruncanella* but is segregated because of the wide chronological gap that separates them. |
| ***Hedbergella*** | Its characters changed so slowly during the Cretaceous that only minor morphological differences developed between H. delrioensis of Albian age and H. holmdelensis of Maastrichtian age. Hedbergella differs from Globuligerina and Fausella by lack of a reticulate ornamentation; from Ticinella by the absence of umbilical supplementary apertures and from Whiteinella by the absence of portici. |
| ***Guembelitria*** | The very small (1500 – 200 microns), triserial test consists of globular chambers. The walls are finely perforate, each pore is surrounded by a blunt cone (sometimes there are two pores per cone). |

**Description:** Test is free, small, biserial, tapering. Chambers globular, rapidly increasing in size; sutures are strongly depressed, giving subtriangular depressions around central sutures. Wall slightly striate. Aperture is an interiomarginal arch at base of last chamber. Maximum length is 260 microns, maximum width 160 microns. Distinguished from *Heterohelix globulosa* by the presence of distinct triangular depressions between the chambers and by being more compressed.

**Stratigraphic range:** Turonian to Santonian (Caron, 1985).

**3. Genus:** ***Hedbergella*** Bronniman and Brown, 1958

**A. Type species**: ***Hedbergella delrioensis*** Carsey, 1979 (Fig. 9)

**Description:** Test is free, trochospiral, biconvex. Equatorial periphery lobulate. Spiral side with 4- 6 chambers in final whorl, gradually increasing in size as added, circular. Sutures are radial and depressed, sometimes slightly curved. Umbilical side has 4-6 globular chambers. Chamber surfaces spinose and papillate, except for the last chamber, which may be smooth. Sutures are radial and depressed. Aperture is an extraumbilical-umbilical arch extending to peripheral margin, with spatulate lip. Umbilicus is narrow 1/6 to 1/5 of maximum diameter of the test. Maximum diameter up to 450 microns, maximum height 200 microns.

**Stratigraphic range:** Middle Aptian to Early Santonian (Caron, 1985)

**B. Type species:** ***Hedbergella planispira*** Tappan, 1979 (Fig. 9)

**Description:** Test is free, very low trochospiral, and appears asymmetrical, with a flat spiral side. Equatorial periphery lobulate with 6-8 chambers in final whorl, which gradually increase in size as added. Sutures are radial and depressed, chambers globular with smooth surface. Umbilical side with 6-8 globular chambers with a smooth surface. Sutures are radial and depressed. Umblicus 1/3 diameter of test. Primary aperture is extraurnbilical-umbilical, extending to periphery, bordered by narrow Hp. Maximum diameter is 21 0 microns, maximum height 80 microns.

**Stratigraphic range:** Albian to Turonian (Robaszynski and Caron, 1979)

**C. Type species:** ***Hedbergella simplex*** Morrow, 1934 (Fig. 9)

**Description:** The species shows great morphological variability particularly in the degree of radial chamber elongation in the last whorl. It is similar to *H. flandrini,* from which it differs in the still stronger and more distinct elongation of the last chamber.

**Stratigraphic range:** Late Cenomanian (Cushman, 1933).

**4. Genus: *Whiteinella*** Pessagno *et al*, 1979
**A. Type species: *Whiteinella archaeocretacea*** Pessagno *et al*, 1979 (Fig. 10)

**Description:** Test free, low trochospiral, chambers oval. Spiral side, equatorial periphery lobulate, sutures depressed, radial and curving forwards in the direction of coiling between chambers. Chambers increase rapidly in size as added and become elongate in the direction of coiling. Umbilical side, 4-5 chambers, sutures radial, depressed, straight, later curving forwards in the direction of coiling. Umbilicus shallow and wide 1/4 to113 of diameter of test. Primary aperture extra-umbilical-umbilical. Portici extending to center of umbilicus. Peripheral border nearly imperforate. Maximum diameter is 400 microns, maximum height 200 microns.
**Stratigraphic range:** Latest Cenomanian to Early Coniacian (Robaszynski and Caron, 1979)

**B. Type species: *Whiteinella baltica*** Douglas and Rankin, 1979 (Fig. 10)

**Description:** Test is free, trochospiral; chambers are circular. Equatorial periphery lobulate. Spiral side has 4- 5 chambers. It is globulose and rapidly increasing in size as added. Umbilical side, 3 and a half to 5 chambers, globose and spinose. Sutures radial and depressed, umbilicus narrow, less than 1/4 of test diameter. Primary aperture is extraumbilical to umbilical bordered by porticus, covering umbilicus. Maximum diameter up to 450 microns, maximum height 200 microns.

**Stratigraphic range:** Albian

**C. Type species: *Whiteinella aprica*** Loeblich and Tappan, 1985 (Fig. 10)

**Table 3:** Distribution and Diversity of Planktonic Foraminiferal Species within the samples analyzed for Microfossils

| Planktonic foraminifera | Sample locations | | |
|---|---|---|---|
| | UEC/Mgbaleze/02 | UEC/Umuezeochie/7 | UEC/Umunama/24 |
| ***Heterohelix reussi*** | 28 | 15 | 9 |
| ***Heterohelix globulosa*** | 7 | 10 | 2 |
| ***Heterohelix moremani*** | 8 | 5 | 21 |
| ***Hedbergella planispira*** | 14 | 8 | 11 |
| ***Hedbergella simplex*** | 1 | 2 | - |
| ***Hedbergella delrioensis*** | 9 | - | 19 |
| ***Guembelitria cenomana*** | - | 21 | 25 |
| ***Guem belitria cretacea*** | - | 5 | 3 |
| ***Whiteinella archeocretacea*** | 2 | 11 | 10 |
| ***Whiteinella aprica*** | - | 2 | - |
| ***Whiteinella baltica*** | 2 | - | 16 |
| ***Whiteinella inornata*** | 2 | - | 1 |
| ***Total species*** | 73 | 79 | 117 |
| ***Species diversity*** | 9 | 9 | 10 |

**Description:** Test is free, low trochospiral consisting of two whorls. Equatorial periphery lobulate. Spiral side 5-7 globulose chambers with pustulose surface, increasing slowly in size as added, sutures radial and depressed. Umbilical side, 5-7 globulose, pustulose chambers. Sutures are radial and depressed, umbilicus shallow and wide up to a 1/4 of the diameter of the test. Aperture is an extraumbilical-umbilical extending towards the periphery, bordered by a porticus. Distinguished from *Whiteinella brittonensis* (Loeblich and Tappan, 1961) by its lower trochospire and flaps in the umbilicus. Maximum diameter 500 microns, height 200 microns.

**Stratigraphic range:** Latest Cenomanian to Late Turonian (Robaszynski and Caron, 1979)

**D. Type species: *Whiteinella inornata*** Bolli, 1957 (Fig. 10)

**Description:** *W. inornata* differs from *W. archaeocretacea*

in the acute and imperforate peripheral margin.
**Stratigraphic range:** Early Turonian (Sigal, 1952)
**Systematic Description of Gastropod Species**
**Family: TURRITELLIDAE** Love´n, 1847
**Genus:** *Turritella* sensu *lato* Lamarck, 1799
**Type species:** *Turritella seriatimgranulata* Roemer, 1849 (Fig. 11)

**Description**: Shell is small, slender. Pleural angle narrow (150). Protoconch and earliest juvenile whorls unknown. Late-juvenile whorls (approximately 1.75 mm diameter) with four (R, A, B, and C) nearly equal and squarish ribs, interspaces deep and smooth and about same width as ribs.

**Stratigraphic range:** Late Aptian to Late Albian.
**Morphological Description of Ostracod**
The recovered species *Clithrocytheridea senegali* (Fig. 11) has a bean-shaped shell with curved anterior margin and more broadly rounded posterior with rounded edges. Its surface is smooth. This is comparable to the forms recovered by Alexander, (2002).

**Stratigraphic range**: Turonian.

## DISCUSSION

### Age and Biostratigraphy

Foraminiferal analysis of the samples yielded four planktonic foraminifera genera, of which Heterohelix followed by Hedbergella are the most abundant, while Whiteinella is scarce to common. Guembelitria is present but less common (Tables 3). The foraminiferal abundance, diversity and recovery was poor.

Whereas the Hedbergellids and Heterohelicids are long ranging, the *Whiteinellas* and *Guembelitirias* are relatively short ranged and have been used together with Turritella to assign Middle-Aptian to Latest-Turonian to the sediments (shales, siltstones, sandstones and limestones) which constitute the lithostratigraphic units in the study area. (Fig. 5). Ostracods are long ranging and thus are not crucial for age dating; in fact, ostracod assemblages in the Late Createceous and Early Palaeogene are similar, and their age is inferred by planktonic foraminifera (Ashu *et al.,* 2015). Whiteinella aprica, and Whiteneilla archaeocretaca species have their bases in the Late Cenomanian and range to Turonian. According to Murray (1991); Robaszynski and Caron (1995), the first occurrence of Whiteinella archaeocretacea clearly marks the Early Turonian. Also recorded in the Early Turonian is the Early Turonian include *Heterohelix pulchra and Heterohelix reussi assemblage (Ehinola, 2010). In addition, the association of Whiteinella inornata, Heterohelix globulosa and Hedbergella planispira has been used to assign a Middle Turonian age (Ehinola, 2010). Guembelitiria cenomana and Guembelitiria cretacea span from Mid- Albian to Early Turonian.*

### Palaeoenvironmental Interpretation

Integrated data from lithofacies and biofacies analyses were used in the palaeo-depositional environment interpretation of the area. Based on the data, a gross lower shelf-shoreface has been interpreted for the area.

Interpretations from lithofacies analysis have shown that several factors controlled sedimentation, hence controlling depositional environment during the times the sediments were being deposited. Figure 13 shows a conceptual block depositional model that displays the spatial relationship of the lithofacies identified in the study area. Continued rise in sea-level led to the deposition of the shales, which is dominant across the area. The grey non-calcareous shales (F 1b-g) sub-lithofacies was deposited in a low energy, relatively low oxygenated conditions, open marine shelf environment, in water-depth probably less than 50 m (Gebhardt, 1997). Nichols (2009) suggests that the formation of dark-grey (or black) shales on shelves occurs provided the supply of organic material is greater than the rate at which it can be broken down. Some physical, biological and chemical factors may have restricted calcareous biofauna to the northern part of the area, thus making calcium carbonate available during deposition. The shale-siltstone (F 2) and shale-sandstone (F 3) interstratification within the area is an indication of sediments deposited at various episodes of relative sea level changes. Reading and Collinson (1996) suggests that the interbedded siltstones and shales indicate equal periods of suspension and bedload deposition with bedload deposition increasing seaward. The heterolithic facies (F 2) and (F 3) suggest storm influenced sediment below the fair-weather wave base, which are typical of lower shoreface (Simpson, 1954 and Amajor, 1987). The Wave ripple laminations are storm generated sedimentary structures formed below fair-weather wave but are typical of lower shoreface sequences (Walker and Plint, 1992). The associated limestone beds with the heteheroliths in the area may be due to periods of low supply of terrigenous clastic detritus and availability of calcium carbonate at that time. The occurrence of burrows of deposit feeders (Chondrites and Planolites) further buttress the shelf-shoreface environment for the sediments (Roy, 1978). The fine-grained sandstones indicate moderate energy environment and sediment influx may have been as a result of wave action.

The poor foraminiferal recovery may be attributed to poor preservation due to long exposure to weathering or age of the rocks and possibly depth of maximum burial. The abundance and diversity of planktonic organisms is controlled by the supply of nutrients and the surface

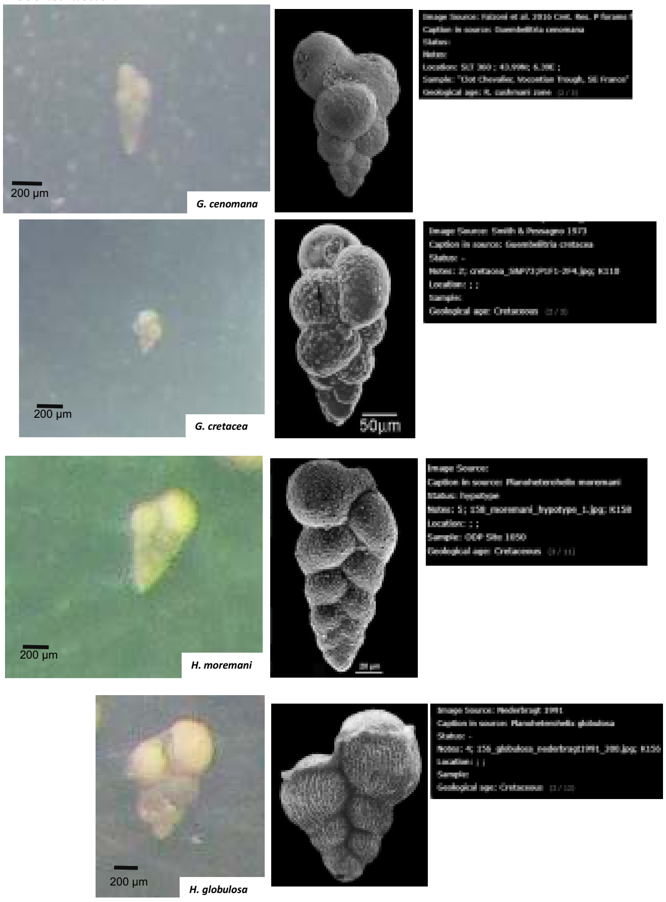


**Figure 8:** Recovered foraminiferal species from Samples analysed **(left column).** Type species of recovered foraminiferal and their sources **(left column)** (image source database: microtax.org/pforams.

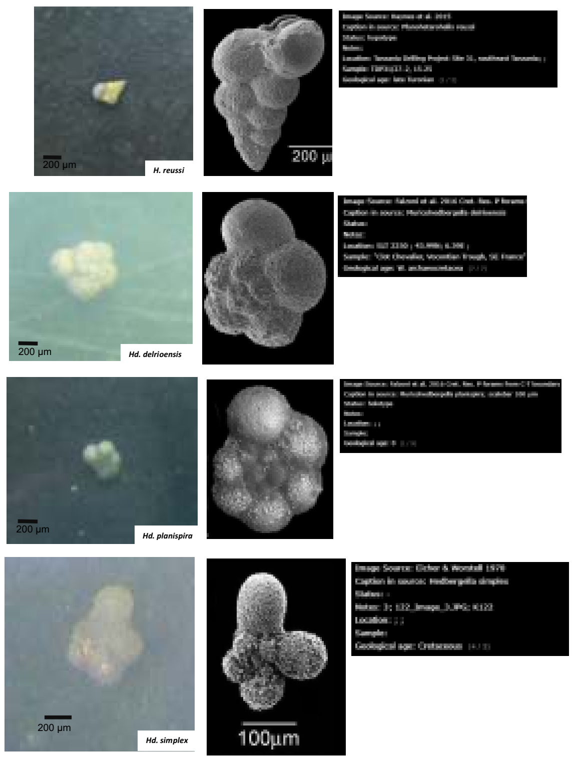


**Figure 9:** Recovered foraminiferal species from Samples analysed **(left column).** Type species of recovered foraminiferal and their sources **(left column)** (image source database: microtax.org/pforams.

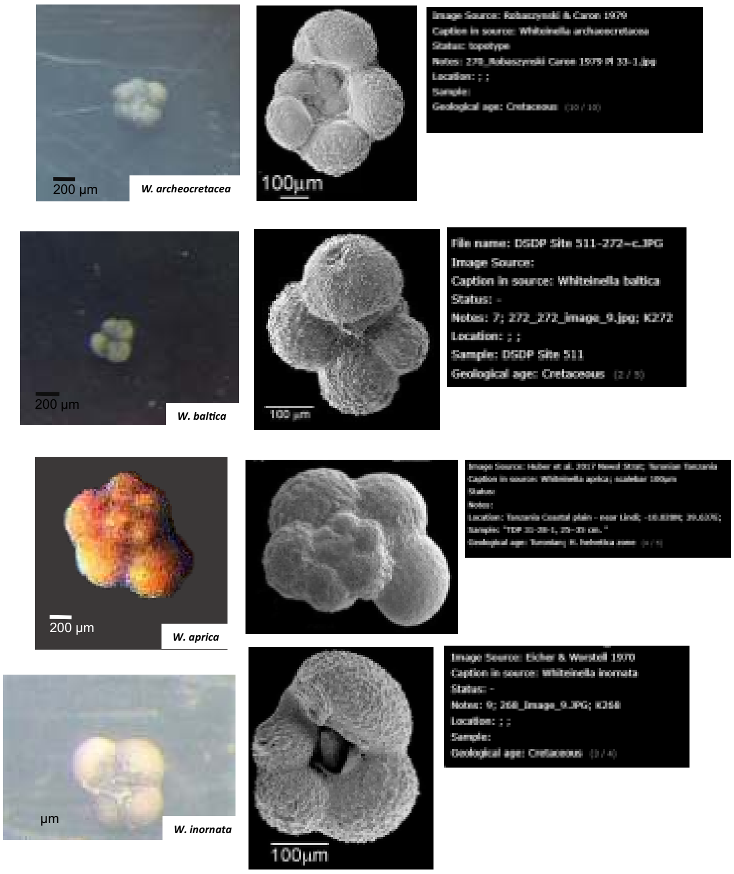


**Figure 10:** Recovered foraminiferal species from Samples analysed **(left column).** Type species of recovered foraminiferal and their sources **(left column)** (image sourcedatabase: microtax.org/pforams).

temperature of the water (Nichols, 2009). Thus, the low abundance and diversity of planktonic foraminifera may be suggestive of unfavourable environmental condition and lack of nutrient supply at that time. Nichols (2009) opined that shoreface environments usually have the most diverse assemblages of benthic fauna and flora due to the well-oxygenated conditions of the wave-agitated water and the availability of light. This implies that overall absence of benthic foraminiferal species in the samples indicates anaerobic bottom water conditions and suggests shallow marine (shoreface) setting.

Heterohelix and Guembelitria are associated with greater depth zones, while species such as Whiteinella baltica is restricted to shallow waters, a fact confirmed by isotopic analysis (Hart, 1999). Guembelitria cretacea and Hedbergella species are linked with warm humid climates, low salinity, temperature and low oxygen conditions (Boersma and Premoli-Silva, 1988; Keller, 1993; Malarkodi *et al.,* 2010). In line with this, Gebhardt (1997) stated that the Turonian marine transgression in Southern Benue Trough are accompanied by lower oxygen levels and possibly, reduced salinities (Gebhardt, 1997). Recent as well as fossil Turritellidae have been studied by stable isotopes (Allmon *et al.,* 1992; Teusch *et al.,* 2002). Recent Turritellidae live in a wide range of environments, mainly shallow infaunal or epifaunal, most commonly in waters less than 100 m deep. They prefer normal marine salinities.

Distribution patterns of Cretaceous planktonic foraminifera are useful for palaeodeposional environment reconstructions, and may reflect temperature gradients of the Cretaceous oceans and epicontinental seas (Berquist, 1969; Douglas, 1972). The absence of Rotaliporids can be explained by the shallow water depth, low thermal gradients, reduced water mass stratification and well developed oxygen minimum zone (OMZ) (Caron and Homewood, 1983; Leckie, 1987). During the Mid to Late Cretaceous, Heterohelicids thrived in low oxygen marine environments with well-developed oxygen minimum zones (OMZ) (Hart and Ball, 1986; Resig, 1993). This corroborates with the view of Odumodu and Mode (2014) that Chondrites-making organisms is influenced more by oxygen deficient conditions. He concluded that Chondrites is reflective of environmental tolerance of oxygen levels lower than any other ichnogenera. Thus, the presence of *Chondrites* in a deposit indicates very low

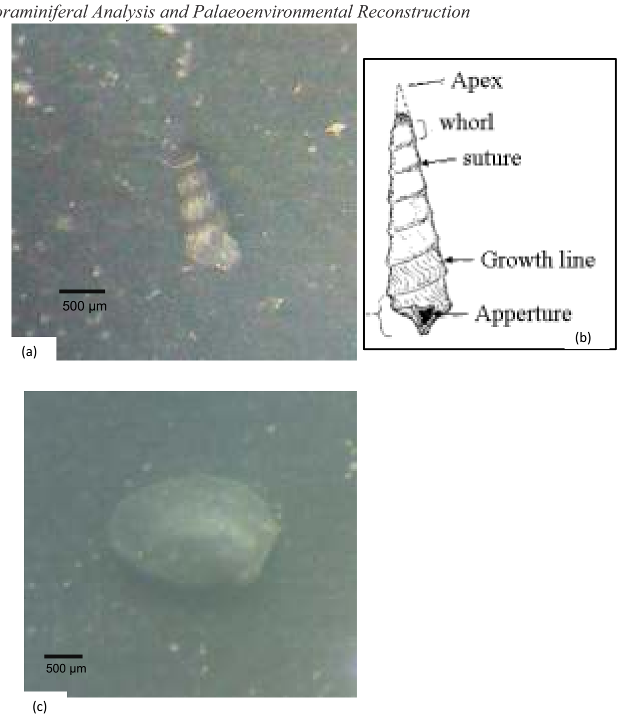


**Figure 11:** (a) Gastropod *Turritella* recovered from analysed sample. **(b)** Sketch gastropod showing names of important of some body **(c)** Ostracod *Clithrocytheridea senegali.*

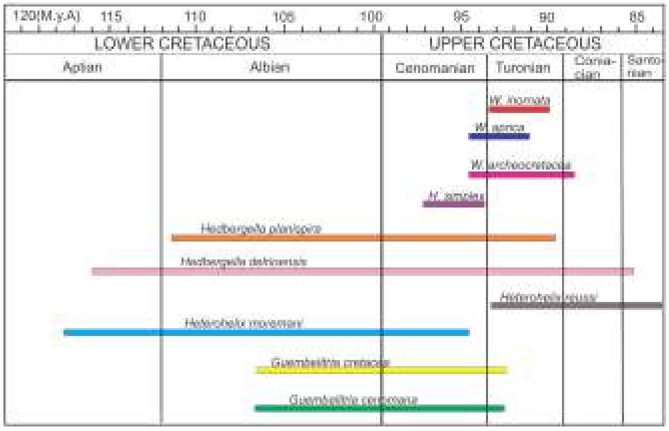


**Figure 12:** Chart showing age ranges for recovered planktonic foraminifera.

oxygen levels (dysoxic conditions) in the interstitial waters within the sediment at the site of burrow emplacement (Bromley and Ekdale, 1984). Open-burrow-fodinichnial traces are maintained by the deposit- feeding organisms (Chondrites and Planolites) to enable them exploit the rich organic matter content of the sediment and at the same time circulating dysoxic water through the burrow for respiration (Martin, 2004). The presence of Planolites within the fine-sandstone suggests reduced salinity, and stressful depositional environment (Durogbitan, 2016). The ostracod species recovered from the area might be more tolerant of reduced oxygen and salt contents (Ehinola, 2010). The low number of individuals and species or non-occurrence of ostracod in the Abakaliki fold belt may be attributed to marine anoxic/dysoxic conditions (Okosun, 1987; Fayose and De Klasz, 1976).

In addition, stable isotope ranking indicates that all Hedbergella species lived in surface or near-surface waters (Price and Hart, 2002), as also indicated by paleogeographic distribution and abundance patterns in open ocean and shallow epeiric sea environments (Hart and Bailey, 1979; Leckie, 1987; Hart, 1999).

**Conceptual Depositional Model**

Integrated lithofacies and biofacies analyses has provided data for generation of a conceptual depositional model for the study area (Fig. 13). The biofacies analysis has helped to constrain the depositional environment to shallow

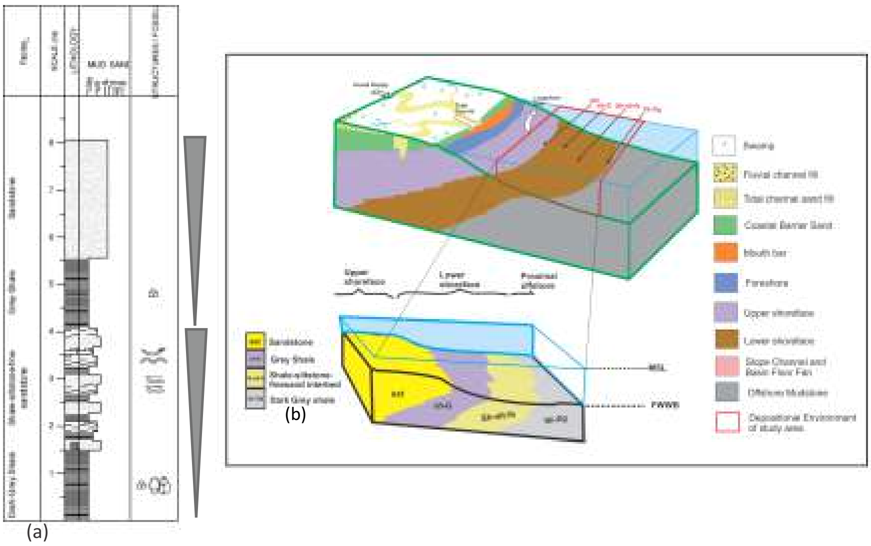


**Figure 13:** (a) Sedimentological log showing the stacked pattern and stratigraphic succession of lithofacies and fossil assemblage across the study area. (b) Conceptual depositional model of the study area.

marine, specifically the lower shoreface. Lithofacies analysis have also provided useful data for interpreting processes that were prevalent during sediment deposition and their environments of deposition. To aid the generation of the model, some of the lithofacies were regrouped based on pattern of deposition of sediment package and colour. The shales lithofacies (F 1) and subordinate lithofacies F 1a and F1b were regrouped into two, namely, dark-grey shale (Sh-Dg) and grey shale (Sh-G). The heterolithic shale-siltstone lithofacies (F 2) and the heterolithic shale-sandstone lithofacies (F 3) were merged as one facies, namely, shale-siltstone-fine sandstone (Sh-Slt-Fs) (Fig. 3).

The depositional sequence in the area began with the deposition of dark-grey shales in a much distal part of the lower shoreface (close to proximal offshore) in a quiet and low energy setting. Alternating periods of moderate and low energy brought in silts and fine sands that formed interbeds and heteroliths with the shales which settled from suspension in the water. A period of increased sea level and low energy setting, but less organic matter, resulted in the deposition of the grey shales in a much shallower depth relative to the dark-grey shales. The low organic matter content may be as a result of increased unfavourable conditions (low saline, stressed and dysoxic setting) for the organisms to thrive. This was followed by an increased energy of the transport medium that resulted in the deposition of the sandstones at the proximal lower shoreface (close the lower/upper shoreface transition area).

## CONCLUSION

Detailed Geologic mapping and lithologic description of outcrop sections in Amofu and the environs indicate that the area is underlain by 4 lithofacies, namely, shale lithofacies (F 1), heterolithic shale-siltstone lithofacies (F 2), heterolithic shale-sandstone lithofacies (F 3), and sandstone lithofacies (F 4). Integrated lithofacies and biofacies analyses provided evidence that the sediments in the area were deposited in shallow marine environment, particularly, the lower shoreface. Data from biofacies further suggest low thermal gradients, reduced water mass stratification, well developed oxygen minimum zone (OMZ), low to normal salinity, low temperature, warm humid climates and bathymetry less than 100 m deep. The beds essentially strike NNE-SSW with dip direction NNW and average dip amount of 200

Based on the fossil assemblage of Whiteinella, Guembelitiria, and gastropod Turritella, the rocks in the study area have been assigned Mid-Aptian to Late Turonian.

## REFERENCES CITED


Alexander, C. I. (2002). Microfossils and paleoenvironment of Numanha Shale of the Upp.er Benue Trough, Northern Nigeria. Journal of Mining and Geology, 8, pp. 57-67.

Allmon W.D., Jones D.S., and Vaughan N., (1992). Observations on the biology of Turritella gonostoma Valenciennes (Prosobranchia: Turritellidae) from the Gulf of California. The Veliger 35(1), pp. 52–63.

Amajor, L.C., (1987). The Eze-Aku sandstone ridges (Turonian) of southeastern Nigeria. A re-interpretation of their Depositional origin. Nigerian Journal of mining and Geology, 23 (1 and 2), pp. 19-26.

Armstrong, H.A. and Brasier, M.D., (2005). Microfossils (zded): Malden. Massachusetts Black well Publishing.

Ashu, Km., Chin, K., Alimohammadin, H. and Dutta, D., (2015). Ostracods, plant tissues, and other inclusions in coprolites from the Late Cretaceous Lameta Formation at Pisdura, India: Taphonomical and palaeoecological implications. Palaeogeography, Palaeoclimatology, Palaeoecology, 418, pp.90-100.

Benkhelil, J., (1982). Benue trough and Benue chain. Geological Magazine, 119(2), pp.155-168.

Benkhelil, J., (1986). Structure and Geodynamic Evolution of the Intracontinental Benue Trough (Nigeria). Ph.D. Thesis, University of Nice. Published by Elf Nigeria Ltd., SNEA (P), pp. 236.

Boersma, A., Premoli-Silva, I., (1988). Atlantic Paleogene biserial heterohelicids and oxygen minima: Paleoceanography, 4, pp. 271-286.

Bolli, H.M., (1957). Planktonic foraminifera from the Oligocene-Miocene Cipero and Lengua formations of Trinidad. BWI Bulletins of the US National Museum, 215, pp. 97-123.

Bromley, R. and Ekdale, A. (1984). Chondrites: A Trace Fossil Indicator of Anoxia in Sediments. Science, 224, 872-874.

Bronnimann, P. and Brown, N.K., (1958). "Taxonomy of the Globotruncanidae": Remarks. micropaleontology, pp. 201-203.

Burke, K., Dessauvagie T.F.W. and Whiteman A.J., (1971). Opening of the Gulf of Guinea and geological history of the Benue Depression and Niger Delta. Nature, Vol. 233, pp. 51–55.

Burke, K., Dessauvagie T.F.W. and Whiteman A.J., (1972). Geological History of the Benue Valley and adjacent Areas. Proceedings of the Conference on African Geology, Vol.s 7–14, pp. 187–205. Published by Department of Geology, University of Ibadan, Ibadan, Nigeria.

Caron, M., (1985). Cretaceous planktonic foraminifera. Plankton stratigraphy, pp.17-86.

Caron, M., and Homewood, P., (1983). Evolution of early planktonic foraminifers. Marine Micropaleontology 7, pp. 453–462.

Carsey, D.O. (1979). Foraminiferas of the Cretaceous of Central Texas. Texas University Bulletin, pp. 2612, 1-56.

Cratchley, C.R. and Jones, G.P., (1965). An interpretation of the geology and gravity anomalies of the Benue Valley, Nigeria. British Overseas Geological Surveys, Geophysics paper, Vol. 1, pp. 1-26.

Cushman, J. A. (1933). Some new foraminiferal genera. Contributions from the Cushman Laboratory for Foraminiferal Research. 9(2): 32-38.

Dim C.I.P., Okwara, C.I., Mode A.W. and Onuoha K.M., (2016). Lithofacies and environments of deposition within the Middle–Upp.er Cretaceous successions of Southeastern Nigeria. Arab Journal of Geosciences vol. 9, pp. 447.

Douglas, R. G., (1972). Paleozoogeography of Late Cretaceous Planktonic Foraminifera in North America. Journal of Foraminiferal Research, 2(1):14-34.

Douglas, R.G. and Rankin, C. (1979). Cretaceous Planktonic Foraminifera from Borhom and their Zoogeographic Significance, Lethaia, 2, pp. 185-217.

Durogbitan A. A., (2016). A Re-evaluation of the Depositional Environments and Sedimentary Facies of Middle Miocene Paralic Deposits (Agbada Formation), Ewan and Oloye Fields, Northwestern Niger Delta. Journal of Marine Science: Research and Development, 6:3.

Ehinola, O. A., (2010). Biostratigraphy and Depositional Environment of the Oil Shale Deposit in the Abakaliki Fold Belt, Southeastern Nigeria. Oil Shale, Vol. 27, No. 2, pp. 99-125.

Ehrenberg C.G., (1978). Verbreitung und Einfluss des mikroskopischen Lebens in sid und Nord Amerika. Abhandlungen der K. preuss. Akademia der Wissen Schaften Phys., -math KI (1841), 1, pp. 291-446.

Ehrenberg, C.G., (1843). Verbreitung und Einfluss des mikroskopischen Lebens in Süd-und Nord-Amerika. Abhandlungen der Königlichen Akademie der Wissenschaften zu Berlin 1841: 291-466, pls 1-4.

Ekwenye, O.C., Nichols, G., Okogbue, C.O. and Mode, A.W., (2016). Trace fossil assemblages in the tide-dominated estuarine system: Ameki Group, south-eastern Nigeria. Journal of African Earth Sciences, 118, pp.284-300.

Fayose, E. A. and De Klasz, I., (1976). Microfossils of the Eze-Aku Formation (Turonian) at Nkalagu quarry, Eastern Nigeria. Journal of Mining and Geology, Vol. 13,(2). pp 51–61.

Gebhardt, H., (1997). Cenomanian to Turonian Foraminifera from Ashaka (NE Nigeria): Quantitative Analysis and Palaeoenvinronmental Interpretation. Cretaceous Res., Vol. 18. P. 17–36.

Grant, N.K., (1971). South Atlantic, Benue Trough and gulf of Guinea Cretaceous Triple Junction. Bulletin of the Geological Society of America, Vol. 82, pp. 2295-2298.

Hart, M. B., Bailey, H. W., Fletcher, S., Price, R. & Swiecicki, A., (l981). Cretaceous. In: Jenkins, D. G. & Murray,J. W. (eds), Stratigraphical atlas of fossil Foraminifera. Ellis Horwood, Chichester, pp. 149-227.

Hart, M.B. and Bailey, H.W., (1979). The distribution of planktonic foraminiferida in the mid-Cretaceous of NW Europe. In: Wiedman, J. (Ed.), Aspekte der Kreide Europas. International Union of Geological Sciences Series A, vol. 6, pp. 527– 542.

Hart, M.B., (1999). The evolution and biodiversity of Cretaceous planktonic foraminiferida. Geobios 32, pp. 247– 255.

Hoque, M., (1976). Significance of textural and petrographic attributes of several Cretaceous sandstones, Southern Nigeria. Geological Society of India, 17(4), pp.514-521.

Keller, G., (1989). Extended Cretaceous/Tertiary boundary extinctions and delayed population change in planktonic foraminifera from Brazos River, Texas. Paleoceanography, 4(3), pp. 287-332.

Keller, G., (1993). The Cretaceous Tertiary boundary transition in the Antarctic Ocean and its global implications: Marine Micropaleontology, 21, pp. 1-45.

Lamarck, J.D., (1799). Prodrome d'une nouvelle classification des coquilles. Mémoires de la Société d'Histoire naturelle de Paris, 1(1), pp.63-90.

Leckie, R.M., (1987). Paleoecology of mid-Cretaceous planktic foraminifera: a comparison of open ocean and epicontinental sea assemblages. Micropaleontology 33, 164–176.

Loeblich Jr, A.R. and Tappan, H., (1961). Suprageneric classification of the Rhizopodea. Journal of Paleontology, pp.245-330.

Loeblich, A.R. and Tappan, H., (1985). Some new and redefined genera and families of agglutinated foraminifera; I. Journal of Foraminiferal Research, 15(2), pp.91-104.

Love´N, S. L., (1847). Malacozoologii. O¨ fversigt af Kongliga Ventenskaps-Akademinens Fo¨rhandlingar, pp. 175–199, pp. 2–6.

Malarkodi, N., Keller, G., Fayazudeen, P.J., and Mallikarjuna, U.B., (2010). Foraminifera from the Early Danian intertrapp.ean beds in Rajahmundry quarries, Andhra Pradesh: Journal of the Geological Society of India, 75, pp. 851-863.

Martin, K. D., (2004). A Re-valuation of the Relationship Between Trace Fossils and Dysoxia. In: Mcllory, D. (ed.) The Application of Ichnology to Palaeoenvironmental and Stratigraphic Analysis. Geological Society, London, Special Publications, 228, 141-156.

Morrow, A.L., 1934. Foraminifera and ostracoda from the Upper Cretaceous of Kansas. Journal of Paleontology, pp.186-205.

Murat, C., (1972). Stratigraphy and Paleogeography of the Cretaceous and Lower Tertiary in South- Eastern Nigeria. In: Dessauvagie, T.F.J. and Whiteman, A.J. (Eds), African Geology. Ibadan University Press, 251–266.

Murray, J. W., (1991). Ecology and distribution of benthic foraminifera. Biology of Foraminifera. Academic Press, London, 221-253.

Nichols, G., (2009). Sedimentology and Stratigraphy. Blackwell Scientific Publications, Oxford, 260 pp.

Nicholson, H.A., (1873). Contributions to the study of the errant annelides of the older Paleozoic rocks. Proceedings of the Royal Society of London, Vol. 21, pp. 288-290, (also Geological Magazine, Vol.. 10, pp. 309-310).

Nwachukwu, S.O., (1972). The tectonic evolution of the the southern portion of the Benue Trough, Nigeria. Geological magazine, 109(5), pp.411-419.

Nwajide, C.S., (2013). Geology of Nigeria's Sedimentary Basins. CSS Bookshops, Lagos. 548 pp.

Obi, G.C., Okogbue, C.O. and Nwajide, C.S., (2001). Evolution of the Enugu Cuesta: a tectonically driven erosional process. Global Journal of Pure and App.lied Sciences, Vol. 7, pp. 321–330.

Odumodu C.F.R. and Mode A.W., (2014). The Palaeoenvironmental

Significance of Chondrites and other Trace Fossils from the Eocene Nanka Formation, Southeastern Nigeria. Journal of Mining and Geology, vol. 50(1), pp. 1-9.

Ofoegbu, C.O., (1984). A Model for the Tectonic Evolution of the Benue Trough of Nigeria. Geologica Rundschau, Vol. 73, pp. 1007-1008.

Ojoh K.A., (1992). The southern part of the Benue Trough (Nigeria) Cretaceous stratigraphy, basin analysis, paleo-oceanography and geodynamic evolution in the equatorial domain of the South Atlantic. Niger Assoc Pet Explor Bull 7(2):131–152.

Okosun, E. A., (1987). Ostracod Biostratigraphy from Nkalagu area in Nigeria. Records of the Geological Survey of 'Nigeria, Vol. 10, 18-31.

Olade, M.A., (1975). Evolution of Nigeria's Benue Trough (Aulacogen): A tectonic model. Geological Magazine. Vol. 112, pp. 575–581.

Pemberton, S. G., MacEachern, J. & Frey, R. (1992). Trace Fossil Facies Models: Environmental and Allostratigraphic Significance. In: Walker, R. and James, N. (Eds) Facies Models: Response to Sea Level Change. Geological Association of Canada, Ottawa, 42-72.

Pessagno Jr, E.A., Finch, W. and Abbott, P.L., (1979). Upper Triassic Radiolaria from the San Hipolito Formation, Baja California. Micropaleontology, pp.160-197.

Price, G.D. and Hart, M.B., (2002). Isotopic evidence for early to mid-Cretaceous ocean temperature variability. Marine Micropaleontology 46, 45– 58.

Reading, H.G. and Collinson, J.D., (1996). Clastic Coasts. Sedimentary Environments: Processes, Facies and Stratigraphy. Blackwells, Cornwall, 154-231.

Resig, J.M., (1993). Cenozoic stratigraphy and paleoceanography of bisrial planktonic foraminifera, Ontong Java Plateau. Proceedings of the Ocean Drilling Program. Scientific Results 130, pp. 231–244.

Reyment, R.A., (1965). Aspects of the Geology of Nigeria. University of Ibadan press, 145 pp.

Richter, R. (1937). Marken und Spuren aus allen Zeiten. 1-11. Senckenbergiana, Vol. 19, pp. 150-169. Sedimentary cycles, South-eastern Nigeria. Sed. Geol. 17, pp. 235–245.

Robaszynski, F. and Caron, M., (1995). Foraminifers planktonique du cretace. Bulletine Society Geological of France, 166, 681-698.

Robaszynski, F. and Caron, M., and the European Working Group on Planktonic Foraminifera, 1979. Atlas of Mid-Cretaceous Planktonic Foraminifera (Boreal Sea and Tethys): Centre National de la Recherche Scientifique, Paris.

Roemer, F. 1849. Texas, mit Besonderer Ru¨cksicht auf Deutsche Auswanderung und die Physischen Verha¨ltnisse des Landes nach Eigener Beobachtung Geschildert. Bonn. 469 pp.

Roy D.J., 1978. The Application of Ichnology to Palaeoenvironmental and Stratigraphic Analysis. Geological Society Special Publication, 228, 314-317.

Short, K.C., and Stauble, A.J. (1967). Outline of geology of Niger Delta. Am. Assoc. Petroleum Geologist Bull.v.51, pp..761-779.

Sigal, J., (1952). Ordre des foraminifera. J. Piveteau (red.), Traite de Paleontologie, pp.209-211.

Simpson, A., (1954). The Nigerian Coalfield: The Geology of parts of Owerri and Benue Provinces. Bulletin of the Geological Survey of Nigeria, No. 24, 85 pp.

Tappan, H., (1979). Microplankton, Ecological Succession and Evolution. N. Am. Paleontol. Conv. Chicago, 1969, Proc. H, 1058-1103.

Teusch K.P., Jones D.J., and Allmon W.D., (2002). Morphological variation in turritellid gastropods from the pleistocene to recent of Chile: association with upwelling intensity. Palaios 17:366– 377.

Tew, B.H. and Mancini, E.A., (1995). An integrated stratigraphic method for paleogeographic reconstruction: examples from the Jackson and Vicksburg Groups of the eastern Gulf Coastal Plain. Palaios, pp.133-153.

Umeji, A.C., (2000). Evolution of the Abakaliki and the Anambra Sedimentary Basins, Southeastern Nigeria. A report submitted to the Shell Petroleum Development Company Ltd., page 155.

Walker, R.G. and Plint, A.G., (1992). Wave- and Storm-Dominated Shallow Marine Systems. In: Walker, R.G. and James, N.P., Eds., Facies Models: Response to Sea Level Change, Geological Association of Canada, GeoText 1, Newfoundland, 219-238.

Wright, J.B. (1968). South Atlantic continental drift and the Benue Trough. Tectonophysics, Vol. 6, pp. 301-310.

NIGERIAN ASSOCIATION OF PETROLEUM EXPLORATIONISTS

SINCE 1975